chemistry

MDPI

Review

Recent Advances in Dynamic DNA Nanodevice

Qin Fan [1], Linzi Yang [1] and Jie Chao [1,2,*]

[1] State Key Laboratory for Organic Electronics & Information Displays (KLOEID), Jiangsu Key Laboratory for Biosensors, Institute of Advanced Materials (IAM) and School of Materials Science and Engineering, Nanjing University of Posts & Telecommunications, Nanjing 210000, China; iamqfan@njupt.edu.cn (Q.F.); iamlzyang@163.com (L.Y.)

[2] Smart Health Big Data Analysis and Location Services Engineering Research Center of Jiangsu Province, School of Geographic and Biologic Information, Nanjing University of Posts & Telecommunications, Nanjing 210000, China

* Correspondence: iamjchao@njupt.edu.cn

Abstract: DNA nanotechnology has been widely used to fabricate precise nanometer-scale machines. In particular, dynamic DNA nanodevices have demonstrated their ability to mimic molecular motions and fluctuations in bion-anomic systems. The elaborately designed DNA nanomachines can conduct a variety of motions and functions with the input of specific commands. A dynamic DNA nanodevice with excellent rigidity and unprecedented processability allows for structural transformation or predictable behavior, showing great potential in tackling single-molecule sensing, drug delivery, molecular systems, and so on. Here, we first briefly introduce the development history of DNA nanotechnology. The driving energy of dynamic DNA nanomachines is also discussed with representative examples. The motor pattern of DNA nanomachines is classified into four parts including translational motion, shear motion, 360° rotation, and complex motion. This review aims to provide an overview of the latest reports on the dynamic DNA nanomachine and give a perspective on their future opportunities.

Keywords: DNA nanotechnology; DNA origami; DNA nanodevice; molecular devices

Citation: Fan, Q.; Yang, L.; Chao, J. Recent Advances in Dynamic DNA Nanodevice. *Chemistry* **2023**, *5*, 1781–1803. https://doi.org/10.3390/chemistry5030122

Academic Editor: Di Li

Received: 30 June 2023
Revised: 31 July 2023
Accepted: 4 August 2023
Published: 10 August 2023

1. Introduction

Artificial nanodevices have advanced significantly in recent years. Nanodevices have proven promising in a number of fields, including nanodrug delivery systems, biosensors, energy, and the environment. Among them, DNA nanodevices play a pivotal role in the development of nanodevices. In the traditional sense, the molecule deoxyribonucleic acid (DNA) is the vehicle in which genetic information is stored and transmitted in most living organisms. DNA has several unique properties, such as being easily available and stable and possessing biosafety. For example, the DNA synthesis process is facile and DNA sequences can be easily customized through gene synthesis, solid-phase chemical synthesis, and biotechnology [1–3]. Compared to RNA and protein molecules, DNA molecules are very stable, and the assembly mechanism of single and double strands has been intensively studied [4–7]. In addition to being a genetic material, DNA can be used to construct nanocarriers or nanomachinces, leveraging its highly programmable nature [8,9]. Delicate DNA structures can be designed and simulated by several design software programs [10–13] including nucleic acid package (NUPACK), graphical integrated development environment for oligonucleotides (GIDEON), tiamat, nanoengineer-1, etc. [14–17]. In addition, DNA is easily modified and functionalized by other chemicals and biomolecules, which makes it an ideal candidate for constructing functional nanomachines [18–20]. In recent years, the rapid development of DNA nanotechnology has enabled many dynamic DNA nanodevices to be designed and constructed, giving rise to various unique and fascinating applications [18,20–22].

The basis of DNA self-assembly originated in 1953, when Watson and Crick discovered the mystery of the double helix of the DNA structure, revealing the existence of the principle of base complementary pairing between DNA molecules [23]. In the 1980s, Seeman discovered that DNA molecules could be used to make programmable multifunctional nanostructures [24,25]. Since then, various DNA nanostructures have emerged one after another. In 2004, Shih et al. used single-stranded DNA (ssDNA) folding to make hollow octahedral structures [26], which established the revolutionary single-stranded DNA origami process, also known as the pre-origami technique. In 2006, Rothemund came up with a potent and straightforward one-pot method called DNA origami, which uses large amounts of short ssDNA (~20–60 nucleotides) to fold long ssDNA (bacteriophage M13mp18 genomic DNA with approximately 7000 nucleotides) into the desired 2D shape. Rothemund uses this technique to fold DNA into shapes such as squares, rectangles, stars, smiley faces, a hemispheric map, etc. [27]. Later, researchers used 2D DNA origami technology to create more complicated DNA nanostructures, including a dolphin [28], polyhedron [29], puzzle [30], and other structures. DNA origami represents a significant breakthrough in DNA nanotechnology, making it possible to construct more complex and sophisticated DNA structures. DNA origami can be used as a model for the formation of crystal superlattices and the construction of inorganic nanostructures due to its exact size and structural diversity [27]. In 2009, Shih and his colleagues expanded DNA origami to build three-dimensional shapes by folding DNA spirals onto cellular lattices. They also developed the caDNAno software program that allows people with no knowledge of programming or DNA structure to quickly learn and complete DNA origami designs [31]. In addition, functional nucleic acids have the potential to artificially construct dynamic nanostructures of functional DNA. As DNA nanotechnology has advanced, DNA structure has developed from the initial static conformation to a structure that can carry out basic conformational transformation and then to the DNA nanostructure, which can complete the preset complex motion. Dynamic DNA nanotechnology involves the dynamic displacement and movement of nanostructures stimulated with the transformation of nucleic acids, such as DNA molecular motors [32,33], DNA walkers [34–36], and DNA detectors [10,37–39]. The design and fabrication of nanodevices with customizable designs and programmable motions are made possible by DNA nanotechnology. Owing to the unique properties of DNA itself, DNA nanodevices have been applied in drug delivery [40–42], catalysis [43,44], nanofabrication [45,46], biological logic gate [47,48], nanophotonics [12,49–51], and other fields.

Herein, our article aims to provide a comprehensive summary of the latest updated research progress of the dynamic DNA nanodevice and explore its future application prospects. We first summarize the two classical DNA assembly techniques for constructing dynamic DNA nanodevices, including DNA origami and DNA tile self-assembly techniques. Subsequently, we introduce the driving forces and the motion mode of the dynamic DNA nanodevices. Finally, challenges and future opportunities in dynamic DNA nanodevices are discussed.

2. Assembly of DNA Nanostructures

DNA origami and DNA tile techniques are the two main methods commonly used to construct dynamic DNA nanodevices with conformational changes. Both of the above two methods are bottom-up strategies, which means that the desired DNA structure can be designed and constructed for specific requirements. In addition, the structural, mechanical, and ionic conductive properties of DNA nanostructures can be predicted by computational software. In addition, it is possible to probe and manipulate dynamic DNA nanostructures with reliable chemical and biochemical tools [18,21,52,53].

2.1. DNA Origami

DNA origami technology represents a highly promising branch of DNA nanotechnology. This approach utilizes lengthy single-stranded DNA scaffolds, typically derived from viral sources and consisting of approximately 7000 nucleotides. These scaffolds are

combined with specifically designed short single-stranded DNA staples, typically composed of ~20–60 nucleotides, to facilitate the folding of DNA molecules, yielding intricate nanostructures in two and three dimensions at the nanoscale [17,46,54,55]. The fundamental idea behind DNA origami design is to convert the desired final shape into the scaffold's folding path and then create staple sequences that can carry out the folding. Software used for designing DNA origami has developed to the third generation, and the commonly used software from one to three generations are caDNAno [56], vHelix15 [57], and ATHENA [58]. The structure, mechanics, and ionic conductivity of DNA origami were simulated by various software programs [14,16,17,59–62].

2.2. DNA Tile

DNA tile assembly is another key technique in DNA self-assembly. Seeman was the first to use the tile method, applying branched DNA molecules with sticky ends to create a 2D crystal structure [18]. DNA tiles are replaced by scaffold-free DNA structures that self-assemble through fundamental interactions. Multiple single-stranded DNA oligomers are self-assembled into a DNA motif, which served as a building block for the subsequent building of complex nanostructures. Each tile typically has one or more crossings, making it stronger.

The structural and mechanical variety of various branched DNA monomers made them suitable for various types of structures in tile-mediated assembly. The DNA tensegrity triangle, multipoint-star motif, and branched DNA with a multihelix as an arm all had fixed interbranch angles and intermolecular tensegrity, making them more likely to be used as tiles in the construction of wireframe structures with clearly defined shapes. The researchers combined flexible ssDNA as vertices with rigid dsDNA to create wireframe structures containing a hollow grid of geometric primitives [63–66].

3. Driving Energy

Since Seeman's group reported the first DNA nanodevice, which depended on structural transitions of DNA driven by small molecules in 1998 [67], dynamic DNA nanomachines have developed rapidly and are evolved into two types including DNA motors and structural switchable DNA nanostructures. The dynamic behaviors of dynamic DNA nanomachines are triggered by specific stimuli, such as the strand displacement reaction, light, electric and magnetic fields, pH, ion concentration, etc., which endow DNA nanostructures with great application potential in sensing, imaging, and drug delivery. In this section, we systematically summarize the latest studies on the driving energy of dynamic DNA nanodevices.

3.1. Strand Displacement Reaction

The DNA strand displacement reaction (SDR) uses a larger stretch of DNA strand (called fuel strand) to displace another weaker-binding sequence from a hybridized DNA double helix structure, a process that takes advantage of differences in the free energy of hybridization of DNA molecules and thus provides precise sequence orthogonality [1]. The motion behavior of complex moving parts in DNA nanostructures can be manipulated with the help of designed strand displacement reactions to construct dynamically deformed DNA nanodevices [68]. The dynamic DNA nanodevices driven by strand displacement reactions can be classified into two distinct categories: Those that undergo conformational changes through this process (e.g., DNA tweezers) and those that achieve device displacement by utilizing strand displacement reactions (e.g., DNA nanowalkers).

The state change of DNA tweezers controlled by strand displacement reactions is one of the typical conformational changes in nanomachines. The representative work is a kind of dsDNA tweezers reported by Yurke and others in 2000, and its principle is joining the fuel strand F and $\overline{F}$ through strands below the reaction control, opening and closing the tweezers. This experiment demonstrated that strand displacement reactions can drive the DNA device to cycle between open and closed states [69]. Accurate conformational transformation and

conformational conduction of DNA nanomachines are important challenges in this field. Ke et al. developed a rhombus-shaped DNA origami "nanoactuator" utilizing mechanical links to replicate distance changes occurring in one half (referred to as the "driver") and transmit them to the other half (referred to as the "mirror") of the device, enabling changes to propagate throughout the system. The motion of the device is regulated by introducing "strut-locking" strands, which form two rigid DNA double helices to control the angles on each side of the diamond structure. Utilizing this nanoactuator, they have developed a DNA-protein hybrid nanostructure incorporating the split enhanced green fluorescent protein (eGFP), demonstrating adjustable fluorescent properties via long-range allosteric regulation [70]. In addition, a specific type of strand displacement reaction called the hybridization chain reaction (HCR) has also been employed in dynamic DNA nanodevices. Chao et al. proposed a DNA navigation system using local chain exchange cascades to search for exits on mazes prefabricated on DNA origami platforms (Figure 1A). Importantly, the two hairpins in the device coexist in a metastable state and provide the necessary power for the PSEC process while allowing storage within their loop regions. The navigator is activated for a random search using DNA hairpin fuels based on the evolution of localized hybridization chain reactions when the ssDNA initiator detects and opens the entry hairpin. The maze comprises five distinct paths, consisting of four dead-ends and a single exit. The navigator has the ability to access all the vertices within the maze. The authors reported a 14.5% success rate in reaching the exit. Subsequently, the author utilizes streptavidin-modified magnetic beads in conjunction with meticulously designed biotin labels to eliminate mazes that follow incorrect paths, resulting in the retention of only the maze with the correct path in the solution [71].

By emulating the movements exhibited by molecular motor proteins observed in living cells, scientific investigators have successfully fabricated a category of devices referred to as DNA nanowalkers. A DNA nanowalker is a typical representative of a DNA nanodevice with a displacement function. Most DNA nanowalkers are driven by strand displacement reactions. The movement of the DNA nanowalkers predominantly relies on toehold-mediated strand displacement. Sherman and Seeman proposed the original DNA Walker model in 2004 (Figure 1B). The system consists of two parts: A footpath composed of a triple crossover (TX) molecule, and a biped region consisting of two double-helical domains connected by three flexible compositions. Each helical domain in the biped has a "foot" at its end, which is a single strand of DNA capable of pairing with complementary DNA strands. A "foothold" is a single-stranded area that exists in each domain of the walkway. The diagram illustrates the movement of the walker, where matching colors indicate complementary DNA strands. By joining the unset strand with the corresponding toehold of set strand binding, then allowing branch migration, which results in the complete hybridization of set strand and unset strand, the corresponding foot is removed from the foothold, and the free foot is connected to the next foothold through the new set strand. Similarly, the other foot moves in the described manner, allowing the Walker to move as a whole [72].

The utilization of additional DNA strands as fuel to propel DNA nanomachines along predetermined orbits has resulted in the development of increasingly intricate and versatile DNA walkers [73]. Lund et al. proposed a random walker called the molecular spider, which comprises a streptavidin molecule as an inert 'body' and three deoxy ribozymes as catalytic 'legs'. The walkers interact with a precisely defined environment and exhibit basic robotic behavior. Based on single-molecule microscopy observations, these walkers employ a two-dimensional DNA origami landscape to detect and modify the paths of substrate molecules. When using specially manufactured DNA origami, the molecular spiders can autonomously carry out activities such as "start", "follow", "turn", and "stop" [36].

The drawbacks of the DNA fuel strand-based DNA nanodevice is the persistent requirement for fuel supplies and the accumulation of waste materials, which lead to a constant alteration in the systems' composition. DNA nanodevices that use light and electromagnetism as driving forces show great possibility of avoiding this problem.

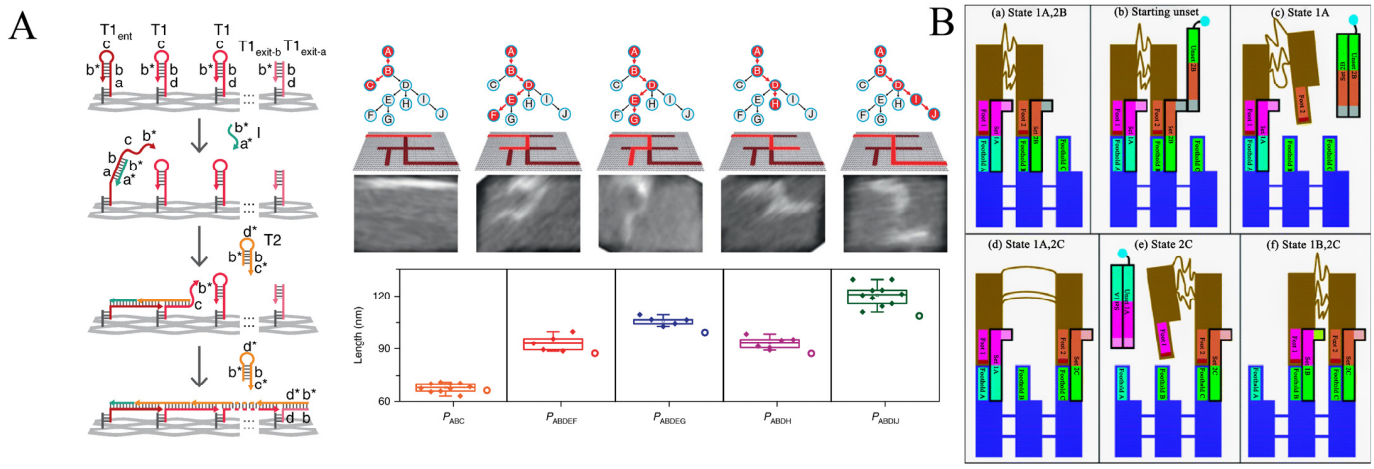

Figure 1. DNA nanodevice driven by strand displacement reaction. (**A**) A DNA navigation system based on localized hybridization chain reactions. Symbols like a and a* represent complementary sequences. Initiator I recognizes and opens the T1ent hairpin at vertex ENT. The opened T1ent hairpin then captures and opens a T2 hairpin from the environment to start the cascade between T2 and T1. Through this mechanism, the navigator can traverse the ten vertices maze, and AFM analysis confirms that the navigator has successfully traveled all possible paths [74]. Copyright 2018, Springer Nature. (**B**) The motion pattern of the original DNA nanowalker model is composed of a footpath and two double-helical domains. The same color in the figure means complementary sequences between strands. (**a**) The initial state of the walker. (**b**) Unset Strand 2B was added to the solution to bind to Set Strand 2B and branch migration occurred. (**c**) Set Strand 2B and Unset Strand 2B were completely hybridized. The walker's Foot 2 is detached from the footpath and is only connected to the footpath through Foot 1 and Set Strand 1A. (**d**) Connect Foot 2 to Foothold C by adding Set Strand 2C, placing the walker in State 1A, 2C. (**e**,**f**) By moving Foot 1 in a similar way to moving Foot 2, the walker is placed in state 1B, 2C [72]. Copy-right 2004, American Chemical Society.

3.2. Light

Light is an excellent energy source for driving the structural deformation of DNA nanodevices, which are equipped with several great properties including cleanness, convenience, and speed [74]. Since DNA itself does not have a light-responsive ability, the construction of photoswitchable DNA nanostructure requires the introduction of photosensitive groups such as photoisomerization molecules, photocage/photocleavage molecules, and photocrosslinking molecules into the DNA sequence [75]. When triggered by light, photosensitive nucleic acid chains could arouse changes in DNA nanostructures, which in turn affect the functional properties of nucleic acids and produce specific biomedical effects.

The photoisomerization process can reversibly control the structural changes of the DNA strands, allowing the strands to switch between two states under the irradiation of light of different wavelengths. Numerous photoisomerization molecules, such as stilbene [76], azobenzene [77,78], and spiropyran [79,80], have been created over time. The most widely used photoresponsive DNA nanodevice is azobenzene because of its self-generated light stability and backward-light modulation between the planar trans and twisted cis state control DNA double-strand stability [81–84]. While the transform lacks an absorbance band in the visible region, the cis form does. Therefore, the right wavelength of light can be selected to ensure the DNA nanostructure is in a stable state with only one azobenzene isomer [74]. For example, Yang et al. revealed a unique photoregulated self-assembly approach for structuring defined regular or irregular DNA architectures made up of photoresponsive DNA origami units (Azo-ODNs). Each origami unit's ability to assemble and disassemble should be controlled by the wavelength-dependent photoinduced isomerization of azobenzene moieties [85]. M. Willner et al. produced DNA nanoscissors that controlled opening and closing using photoresponsive DNA oligonucleotides

containing azobenzene molecules and switched reversible opening/closing states of the nanoscissors via ultraviolet and visible light irradiation (Figure 2A). The same principle is also used to manufacture a square component with four photofunctional units that can take either square or diamond fold forms [86].

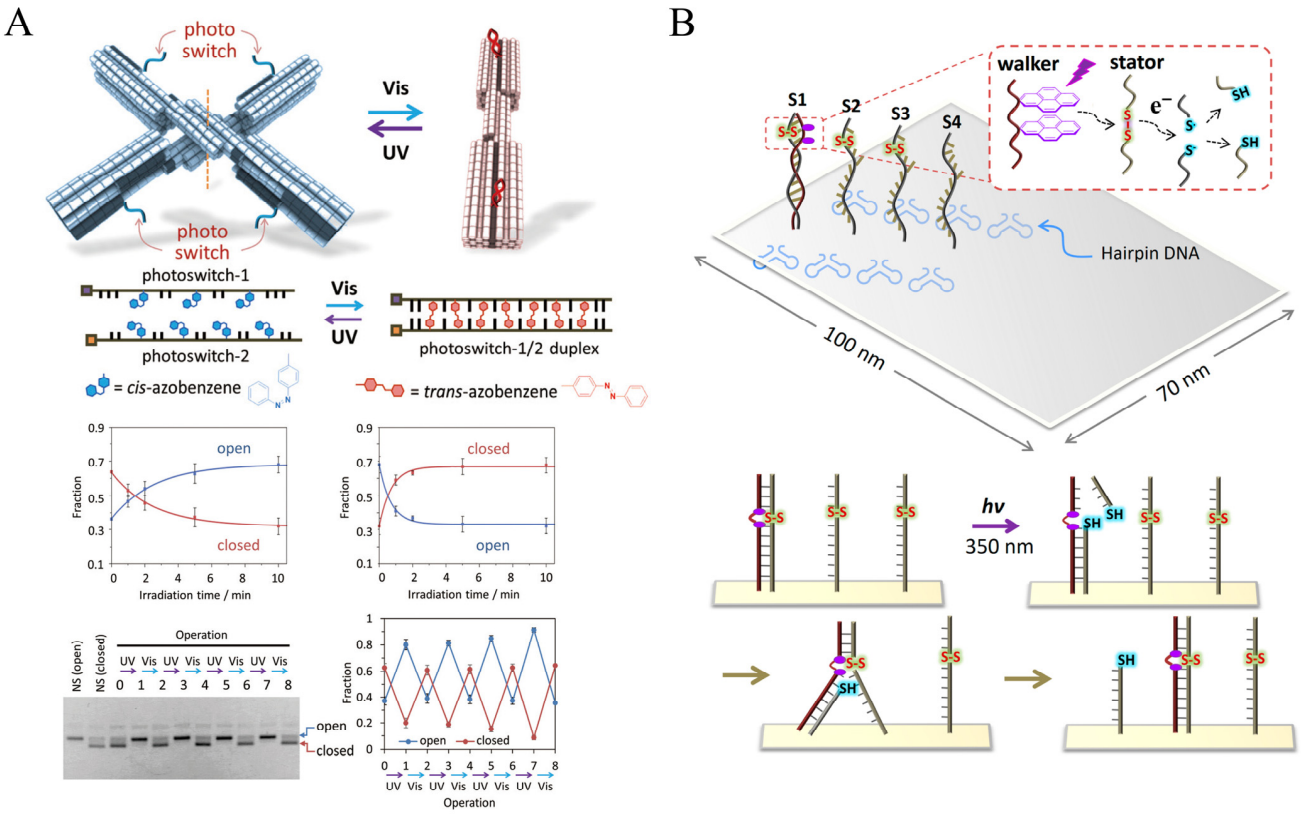

Figure 2. Photoactuation of DNA nanodevice. (**A**) Photoresponsive DNA nanoscissors were fabricated using photoresponsive DNA oligonucleotides containing azobenzene molecules [86]. Copyright 2017, John Wiley and Sons. (**B**) A Light-driven DNA walker consists of stator strands connected by disulfide bonds and walking strands modified with pyrene [84]. Copyright 2015, American Chemical Society.

Another class of components used to build photoswitchable DNA nanostructures is primarily photocleavable/photocaged molecules, which refer to a series of molecules that can be photocleaved. Photocage compounds are photocleavage groups embedded in key positions of nucleic acid sequences that temporarily inactivate the biological activity of the nucleic acid. Upon stimulation by light, it disrupts the connection between the photocage moiety and the DNA, allowing the function of the nucleic acid to be restored. Photocleavage compounds typically utilize covalent bonds to link two or more nucleic acid sequences. Upon light irradiation, the bonds of the photocleaved molecule are broken and the nucleic acid sequence is cleaved into smaller fragments, thus restoring its corresponding functions. Photocleavage/photocage molecules have been widely used to regulate the hybridization of nucleic acids and can confer on/off behavior of DNA nanostructures, becoming a major direction in the construction of dynamic DNA nanostructures. By leveraging this mechanism, Yang et al. described a light-driven DNA nanodevice in 2015, which can move along a single 2D DNA tile's linear track (Figure 2B). The 2D DNA tile was put together using stator strands connected by disulfide bonds and walking strands modified with pyrene as anchorage sites to allow walker motion. The pyrene molecules activated by photoirradiation at 350 nm caused the cleavage of disulfide bond-connected stator strands, allowing the DNA walker to migrate from one cleaved stator to the next on the DNA tile [84].

Photocrosslinking molecules are commonly used to build or stabilize DNA nanostructures. The photocrosslinking group reacts with the corresponding groups of the nucleic acid bases in a photocrosslinking reaction, allowing the ends of two neighboring strands to be joined together. Reversible photoresponsive nucleic acid cross-linking enables the modulation of the nucleic acid structure and sequence-specific detection. Kandatsu and coworkers designed an X-shaped DNA sequence with the photocrosslinking group 3-cyanovinylcarbazole (CNVK) introduced at the tip of each arm. This gel achieves repetitive sol-to-gel and gel-to-sol transitions when driven by UV radiation at different wavelengths and temperatures [87].

Despite the advantages associated with light-responsive systems, there are still limitations that must be addressed. One notable challenge is the limited penetration depth of ultraviolet (UV) radiation, which makes it difficult to apply photoactuation techniques in in vivo contexts [88]. Furthermore, high doses of UV irradiation can lead to the destruction of the DNA backbone, while low UV doses are insufficient to activate the photosensitive units. Additionally, endogenous thiols present in cells, including glutathione (GSH), have been found to reduce azo compounds [89,90].

3.3. Electric and Magnetic Fields

The utilization of electric and magnetic fields for controlling motion in DNA nanodevices showed unparalleled response speed and precise control ability, which is significantly different from SDR-driving motion. Currently, electric and magnetic fields are predominantly employed in DNA nanodevices to induce rotational and translational motion [91–93].

Electrically charged DNA nanostructures can be manipulated by external electric fields for rapid response and precise space-time control. An electric field-controlled DNA nanodevice system was proposed by Kopperger et al. [92]. The actuator unit of the system consists of a DNA origami board and a DNA origami robotic arm. The arm was connected to the tile through ssDNA scaffold crossings, and the flexible joint facilitated stochastic switching of the arm due to transitory binding. With two pairs of platinum electrodes inserted into each of the four buffer reservoirs, two parallel fluid channels come together to form a cross chamber. The fields generated by the electrode pairs are applied to immobilized DNA nanostructures in the cross chamber. Therefore, voltage can be applied to control the arm's pointing direction arbitrarily. According to reports, this DNA robotic arm is at least five orders of magnitude faster than earlier DNA motor systems and belongs to the same category as biohybrid motors powered by adenosine triphosphatase. A synthetic tubular molecular transport system was proposed by Stömmer et al. (Figure 3A). The hollow pipe allows the natural molecular piston to move in the form of diffusion within the pipe, and the applied electric field can accelerate the piston motion to upgrade the system to an electric rail system. Under the condition of adding an electric field, piston velocity can reach 9 μm/s [94].

The inherent negative charge of DNA enables DNA nanomachines to be directly propelled by external electric fields. In contrast, magnetic field-driven DNA nanomachines operate under different principles, typically necessitating the attachment of magnetic particles for propulsion in external magnetic fields [91]. Directly manipulating molecular-scale devices by manipulating micron-sized magnetic particles via externally provided magnetic fields is challenging due to higher thermal fluctuations and lower forces resulting from scaling down magnetic particles. Lauback et al. devised a different way to modulate DNA origami motion using an external magnetic field (Figure 3B). The rotor structure consists of a platform, a rigid rotating arm, and a micromagnetic bead positioned at the distal axis end of the arm. The rotor binds to the base platform surface through biotin-streptavidin affinity. The system enabled accurate control (8° precision) of the angular conformation, and unremitting rotational motion (up to 2 Hz). This nanodevice torque application is up to 80 pNm [95].

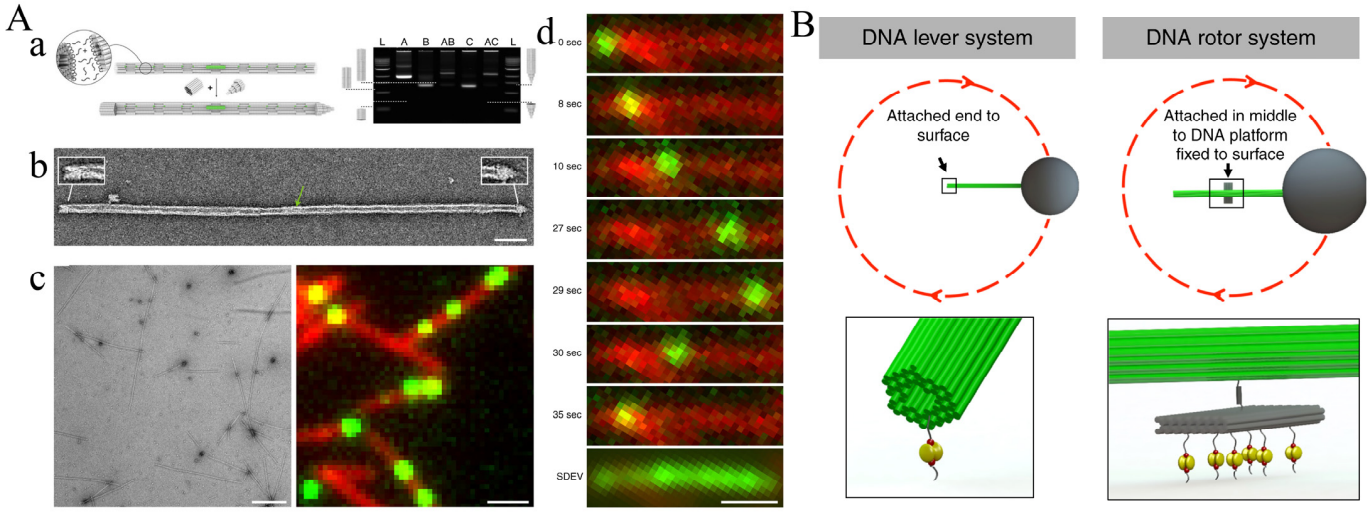

Figure 3. Electric and magnetic actuation of DNA nanodevice. (**A**) A DNA tubular transport system accelerated by an applied electric field. (**a**) **Left**: Assembly diagram of tubular molecular transport system, **Right**: gel-electrophoretic analyses of each component. (**b**) Exemplary negative-staining TEM image of a capped filament. (**c**) Left: Typical field of view negatively stained TEM image of polymerized filaments. Right: Typical field of view TIRF image of polymerized filaments (modified Cyanine-5 dyes) with piston objects trapped inside. (**d**) Sequence of individual frames extracted from a total internal reflection fluorescence (TIRF) movie illustrates the dynamic motion of a piston along a filament [94]. Copyright 2021, Springer Nature. (**B**) DNA lever system and DNA rotor system driven by magnetic field are both composed of 56 helix nano-brick, nano-rotor and nano-hinge. In the system, micromagnetic beads are connected to the distal axis of the arm. The rotating parts are connected to the surface by biotin-streptavidin affinity [95]. Copyright 2018, Springer Nature.

3.4. pH

Various organs exhibit different pH characteristics. For instance, healthy tissue maintains a neutral pH environment (pH 7.4), cancer cells are surrounded by a mildly acidic microenvironment (pH 6.5–7.2), and lysosomes and exosomes demonstrate an acidic state (approximately 5.0) [90,96]. Tissue pH abnormalities are frequently associated with diseases. Consequently, researching pH-responsive DNA nanodevices holds significant implications for drug transportation and disease diagnosis. The pH-responsive dynamic DNA nanodevice generally contains pH-sensitive nucleic acid strands, which could experience cyclic and reversible structural changes brought on by pH changes [74]. The i-motif structure is a major part of the pH-responsive DNA sequence. Under acidic conditions (pH 5.0), cytosine-rich sequences self-assemble into i-motif structures that separate under neutral circumstances. Similar to how Hoogsteen type C-G·C^+ bridges in triplex-DNA structures stabilize under acidic conditions and separate under neutral conditions, T−A·T bridges in triplex strands stabilize at neutral pH and separate under basic conditions [97–101]. R. Burns et al. assembled a hexahedron with a [3,4]-fold symmetry topology using DNA origami techniques (Figure 4A). By modifying the outer surface of the hexahedral device with the HIV-Tat transduction domain, the device functions as an everted virus. The device features a lid controlled by i-motif strands, which opens when the pH is reduced from neutral to 6. Enabled by this distinctive design, the device can effectively deliver proteins into living cells [19].

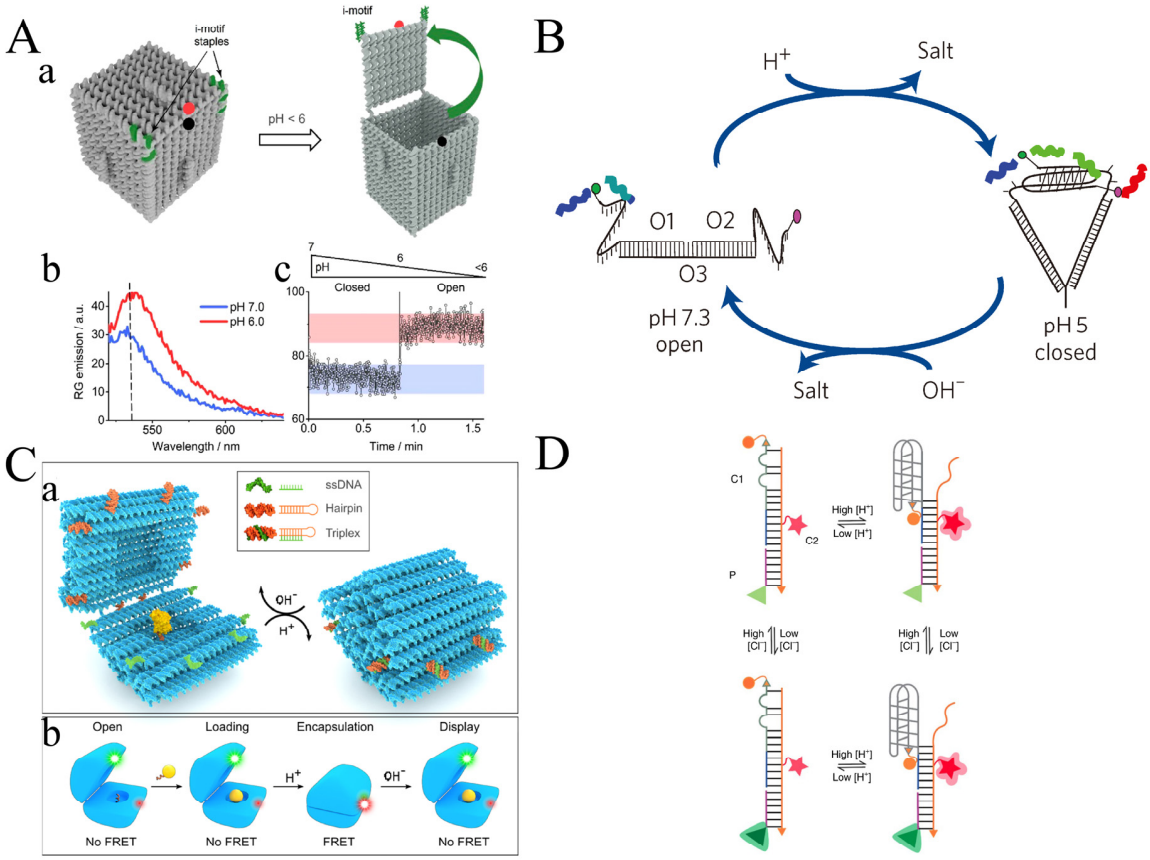

Figure 4. Proton actuation of DDAs of DNA nanodevice. (**A**) An i-motif Sta-ple-controlled everted-virus topology for the virus functional protein delivery. (**a**) The device is regulated for its opening and closing mechanisms by i-motif staples (represented in green). The box is designed to open in response to a decrease in pH. Reporter (rhodamine G, RG) and quencher (dabcyl) are shown in red and black. (**b**) The device has demonstrated significantly distinct FRET spectra in closed state (pH=7) and open state (pH = 6). (**c**) The pH-induced device closed to open is plotted versus time in a FRET spectra [19]. Copyright 2018, American Chemical Society. (**B**) A DNA nanodevice called "I-switch" served as a sensor to track both the temporal and spatial pH variations in living cells. By specially designed fluorescent labeling I-switch in the 'open' state (low FRET) at high pH and in the 'closed' state (high FRET) at low pH [102]. Copyright 2009, Springer Nature. (**C**) Reconfigurable DNA origami nanocapsule for pH-controlled encapsulation and display of cargo. (**a**) A cargo-carrying DNA origami nanocapsule can change the open-close states of the pH-latch structure by responding to the pH changes of the surrounding fluid. (**b**) The upper and lower half modified fluorophore represent the on-off state of the nanodevice by FRET [52]. Copyright 2019, American Chemical Society. (**D**) A device that uses double-stimulated DNA that can quantitatively measure pH and the chloride ion (Cl^-) in lysosomes at the same time. This device quantitatively measures pH levels by utilizing the fluorescence resonance energy transfer (FRET) phenomenon between Alexa 546 (acting as the donor, represented by an orange sphere) and Alexa 647 (acting as the acceptor, represented by a red star). Additionally, Cl^- concentration is determined using a chloride-sensitive fluorophore (BAC, depicted as a green triangle) in conjunction with Alexa 647 [39]. Copyright 2018, Springer Nature.

Yamuna Krishnan's research group described a DNA nanodevice called "I-switch", which served as a sensor to track both the temporal and spatial pH variations in living cells (Figure 4B) [39,102]. This pH sensor displayed an "open" state when the pH level was high. Proton activation of two cytosine-rich regions in the DNA nanodevice leads to the formation of an i-tetraplex, causing a structural transition from a linear conformation to a closed tweezer-like state. Due to its response time of 1 to 2 min and its ability to detect pH changes between pH 5.5 and 6.8, this sensor is ideal for monitoring intracellular

pH variations [102]. Yamuna Krishnan's research group utilized the "I-switch" device in both wild-type and mutant worms, employing fluorescence resonance energy transfer to accurately map the spatio-temporal pH changes associated with entosis. This approach unveils autonomous functions within the organism's environment across various genetic contexts [103].

In addition, pH-latch structures are also used for pH-responsive DNA nanodevices [52]. Ijas et al. used DNA origami to create a DNA nanodevice for cargo transport that can be switched on and off depending on pH, which the authors call the nanocapsule (Figure 4C). A central part of its pH response is the "pH-latches", which are made up of double-stranded and single-stranded DNA. At lower pH, single-stranded DNA and hairpin DNA form a parallel triplex DNA structure, at which point the nanocapsule is closed, and at higher pH, the two strands separate and the nanocapsule is open. The device has an extremely fast response time and is sensitive to pH changes, with an increase of approximately 0.5 pH units allowing the sample to switch from closed to open. Through experiments, the researchers proved that the nanocapsule has a good shielding effect on the cargo carried [52]

In recent years, multi-responsive DNA structures for complex physiological environments have also been invented. A double-stimulated DNA device was created by Leung et al. that can quantitatively image pH and Cl^- in the lysosomes at the same time (Figure 4D). Analyzing two ion measurement (2-IM) profiling of the lysosome allowed for highly efficient and accurate reflection of the H^+ and Cl^- levels. This method shows promise in objectively identifying potential lead compounds for Niemann–Pick diseases to identify potential patient cohorts for clinical trials, track the effectiveness of treatments, or monitor disease progression [39].

pH-sensitive nanodevices have the potential to detect pH, diagnose specific diseases, and facilitate in vivo drug delivery. However, the instability of DNA under strong acids and bases imposes limitations on its range of applications. In future research, it is still necessary to improve the comprehensive study of the dynamics of the pH-responsive DNA chains.

3.5. Ions

Ion-driven dynamic DNA nanostructures contain two main types. The first is electrostatic repulsion induced by the negatively charged phosphate backbone under cationic conditions. Marras et al. assembled cation-responsive reconfigurable DNA origami capable of rapid response at millisecond scales (Figure 5A). The method relies on the ion-mediated hybridization of multiple short single-stranded DNA strands within the device. This method utilizes multi-valent interactions driven by weak DNA base-pairing, which are highly sensitive to local ion concentrations. Consequently, device reconfiguration is achieved without the necessity of binding DNA components from the solution or displacing DNA strands. The research team investigated the impact of monovalent, bivalent, and trivalent ions on the behavior of the device. They observed that higher ion valence significantly enhances the device's sensitivity to actuation, and the ratio of the closed state shows a positive correlation with ion concentration [104].

The second ion actuation relies on ion-stimulated molecules [90]. Linear G-rich telomeric DNA strands are frequently employed in cation-responsive structures. They fold into G-quadruplex structures when certain cations (K^+, Na^+) are present. Upon removal of the cationic environment, they transition back to their initial structure from the folded state [105,106]. A G-quadruplex structure is formed by the stacking of G-quartets, which are planar ring structures stabilized by Hoogsteen bonds among four guanine bases that can be contributed to by one, two, or four independent nucleic acid strands. The G-quadruplex can be stabilized by the O6 atoms of guanine bases in G-quartets, as well as metal ions [90,106,107]. In addition, the researchers incorporated non-native heterocyclic bases into the oligonucleotide strands (ligandosides) as chelators for metal ions, including Cu^{2+} ions, which facilitate nucleic acid structure bridging [108–110]. Furthermore, they investigated the bridging of mismatched duplexes by metal ions, such as T-T or C-C mis-

matched sequences bridged by Hg^{2+} or Ag^{+}, and the subsequent separation using thiolated ligands [74,111–113].

Kuzuya et al. proposed an ion detection clamp that uses G-quadruplex formation for Na^{+} detection (Figure 5B). After the addition of Na^{+}, the proportion of antiparallel DNA clamp increased, and the proportion of the cross-form clamp decreased. The equilibrium time after the addition of Na^{+} was approximately 2–3 h. In the presence of K^{+}, the TeloE sequence is also known to dimerize. In addition, the researchers mediated selective stabilization of C-C mismatches to Ag^{+} ions, and 47% of the tweezers became parallel when Ag^{+} was added [114].

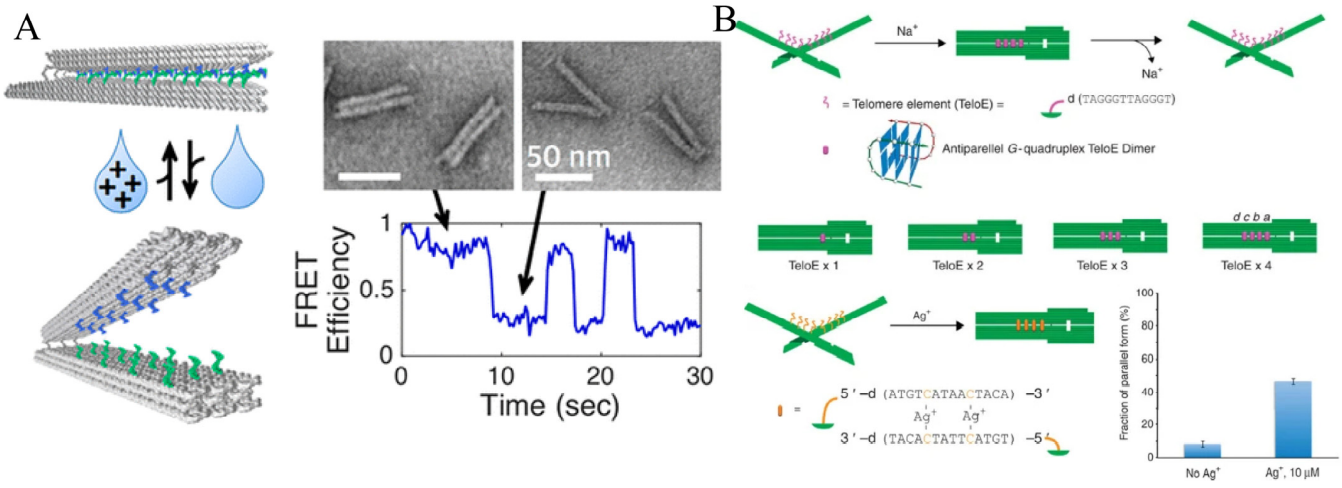

Figure 5. Ion actuation of DNA nanodevice. (**A**) Through the ion-mediated hybridization of multiple short single-stranded DNA strands within the device, a cation-responsive DNA origami demonstrates millisecond-scale responsiveness and the ability to be quickly reconfigured [104]. Copyright 2018, American Chemical Society. (**B**) Ion detection clamp is used to detect Na^{+} by Na^{+}-triggered zipping of DNA pliers bearing a G-quadruplex zipper. Ag^{+} was detected using DNA pliers bearing C-C mismatched zipper elements [114]. Copyright 2011, Springer Nature.

In addition, the ion-dependent DNAzyme is another ion-stimulated molecule that could cleave the phosphodiester skeleton at nucleotide or deoxynucleotide sites. So far, researchers have developed several DNAzymes special for Ag^{+}, Pb^{2+}, Zn^{2+}, and so on. Leveraging the DNAzyme-dependent strategy can be used for constructing ion-sensitive DNA nanodevices [115,116]. Wu et al. reported DNAzyme-controlled cleavage of dimer and trimer origami tiles. In this system, a DNA origami tile modified with Pb^{2+} and histidine-dependent DNAzyme can manipulate the dissociation of dimers and trimers by controlling the addition of Pb^{2+} and histidine.

Ion-sensitive nanodevices can be used as ion concentration sensors because they respond quickly to different ion concentrations or different ions. However, it is difficult for DNA nanostructures to maintain stable morphology at a low ion concentration, and most ion responses require external manual adjustment of concentration, so their application scope is limited. Its applications are usually in vitro for ion concentration detection and ion-driven structural changes in DNA nanodevices.

In addition to the above methods, temperature [117,118], fluidic flow [33], and enzymes [119] can be used as energy sources for the DNA nanodevice. In addition, researchers have developed DNA nanodevices that operate with no energy and rely solely on Brownian motion [120].

4. Motor Pattern

From a broad perspective, motion encompasses the changes in an object's position or orientation over time. The primary and ubiquitous forms of motion consist of translational and rotational motion. Motion in DNA nanodevices is commonly classified as translational, rotational, or a complex combination of both—complex motion [121]. Here, rotational motion is subdivided into two types. One is the motion of two or more parts rotating < 360° around an axis in the DNA nanodevice system, which is called shear motion. The second type is a machine that can rotate 360° about its axis, and the mode of motion is called 360° rotation.

4.1. Translational Motion

Translation motion is one of the simplest motion modes, and most of the motion modes of DNA walkers belong to translation motion. Cha et al. proposed a motor based on RNA-cleaving DNA enzymes that can transport nanoparticle cargoes along single-walled carbon nanotubes (Figure 6A). These motors draw chemical energy from the nanotube-decorated RNA molecules and use that energy to power autonomous, processive walking along a one-dimensional track by undergoing a series of conformational changes. Due to the inherent controllability and adaptability of walking, people are able to remotely command actions such as "go" and "stop" in response to changes in the immediate environment. The nanotube motion machine can achieve one-dimensional motion, and the motion mode is also a translation motion [122].

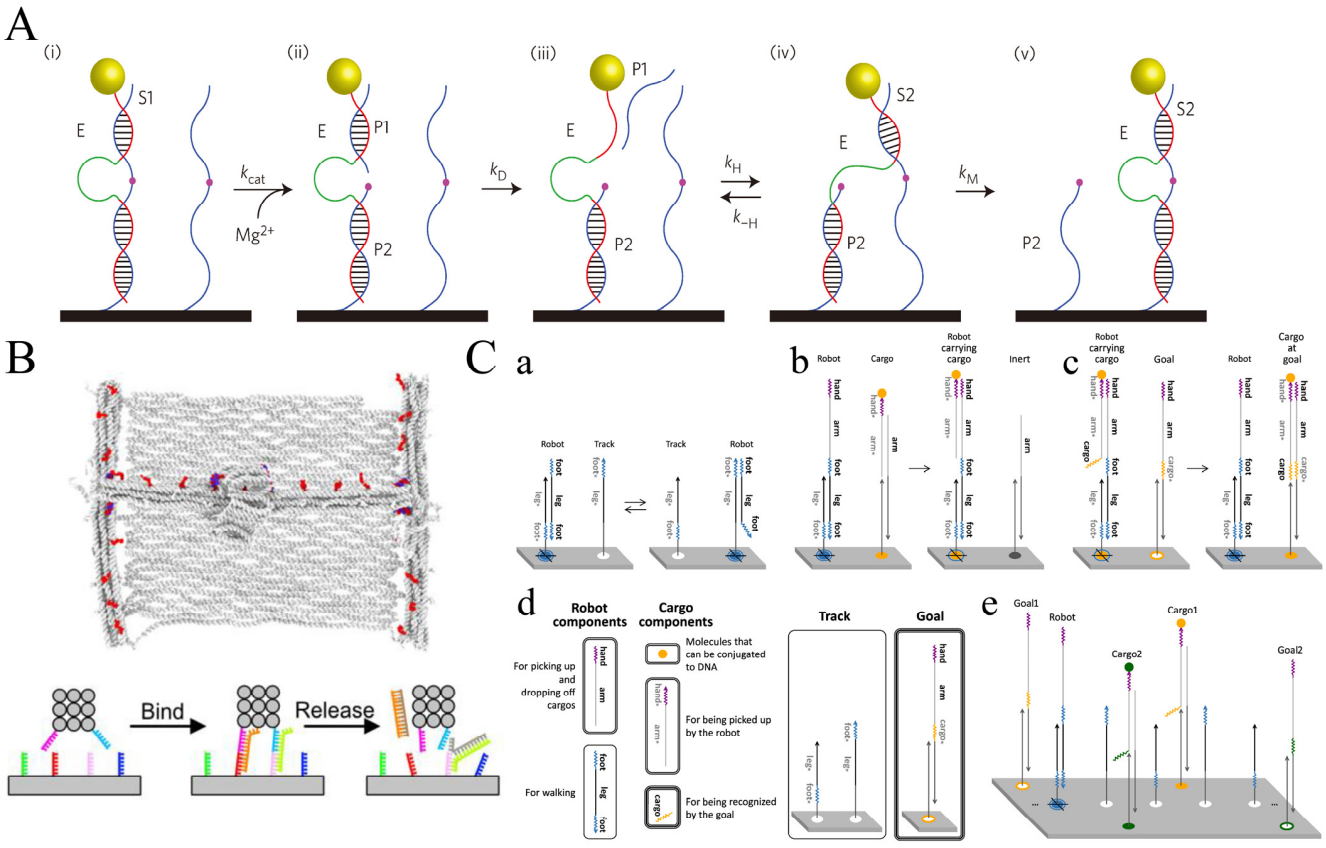

Figure 6. Translational motion of nanodevices. (**A**) Nanoparticle payloads can be transported over single-walled carbon nanotubes using a motor based on DNA enzymes that break down RNA. (**i–v**) The working principle of the DNAzyme-based motor. DNAzyme (E), after binding to RNA (S1), Cut S1 (pink) in the presence of Mg2+, producing short (P1) and long (P2) fragments. P1 then dissociates

from E, and the unbound recognition arm of E associates with an adjacent RNA (S2) on the track. The molecular motor moves along the nanotube orbit based on repeating this process [122]. Copyright 2013, Springer Nature. (**B**) A DNA molecular printer driven by strand displacement reactions with programmable positioning and the ability to generate two-dimensional patterns [123]. Copyright 2022, American Association for the Advancement of Science. (**C**) A robot that can classify goods on a two-dimensional plane can display (**a**) random walk, (**b**) cargo pickup, and (**c**) cargo drop-off, and can (**d**) combine three modules to (**e**) achieve multiple types of cargo sorting [35]. Copyright 2017, American Association for the Advancement of Science.

In addition to DNA nanodevices capable of one-dimensional movement, scientists have also developed nanodevices that can move in two dimensions. Recently, Benson et al. proposed a DNA molecular printer with programmable positioning and two-dimensional patterns (Figure 6B). This device is made by combining three separately programmable DNA origami linear actuators. The system consists of a moveable gantry that threads a mobile sleeve while traveling along parallel rails. By adding signaling oligonucleotides, this device is able to reversibly position a write head over a canvas. By using the head to catalyze a local DNA strand-exchange reaction, the "write" functionality can modify specific pixels on a canvas. The sleeve and the writing head above can move in x and y directions, thus meeting the conditions of translational motion [123]. J. Thubagere et al. proposed a robot that can use three modules (random walk, cargo pickup, and cargo drop-off) to sort cargo on 2D DNA origami according to a simple algorithm (Figure 6C). The robot can move the unordered cargo to a specific location until all the cargo is divided into two different piles. The robot can walk randomly without any energy supply and repeatedly classify multiple cargos. Its motion mode is translation motion on a 2D plane [35].

4.2. Shear Motion

Shear motion is one of the motion modes commonly used by DNA nanodevices, which is applied in the fields of force spectrometer [124], drug delivery [42,125], and optical properties generation [12,126]. Shear motion is driven by a variety of energies, including temperature [118], ion concentration [86,104], strand displacement [50,70,126,127], light [75,86], electric [128], drive, etc. Kuzyk et al. reported reconfigurable 3D plasmonic metamolecules (Figure 7A), which consist of two origami bundles connected with AuNR, and the system uses DNA locks and fuel strands to make conformational changes in situ into circular dichroism changes in the visible wavelength range [12]. Zhan et al. constructed a reconfigurable DNA origami tripod using the DNA self-assembly technique and placed three gold nanorods on the tripod, which can adjust the angle and distance of the nanorods by toehold-mediated strand displacement (Figure 7B). Single-Structure Dark-Field Scattering Spectroscopy was studied, and it was proven that the peak splitting of dark-field Scattering Spectroscopy between nanorods became more obvious when the angle was larger [126].

In addition to its applications in nanophotonics and nanoelectronics, shear motion is frequently utilized in various drug delivery devices [42,125,129], reaction control devices [127], and DNA origami switches [114,130]. Grossi et al. introduced a DNA origami device called the DNA Vault (DV) (Figure 7C). Five double-helix locks were installed on the front, sides, and hinge, together with two hairpin locks to govern how the DV opened and closed. These locks on the DV can be switched on and off by DNA strand displacement with a key. DV is used to control the enzymatic reaction catalyzed by an electrolyte protease [127]. In addition to base complementation, shape complementation can also be used to design DNA origami switches that perform scissor-like motions. Gerling et al. proposed a DNA origami switch based on this principle (Figure 7D). The switch can be changed from an open state to a closed state when the cation concentration is increased or heated, and the open state can be restored when the concentration decreases or the temperature is lowered. The researchers strategically positioned ssDNA loops near the shape-complementary interfaces in both the switch and the dimeric brick objects. Specifi-

cally, in the switch, toehold-mediated DNA strand displacement was employed to precisely regulate the switching on and off dynamics [130].

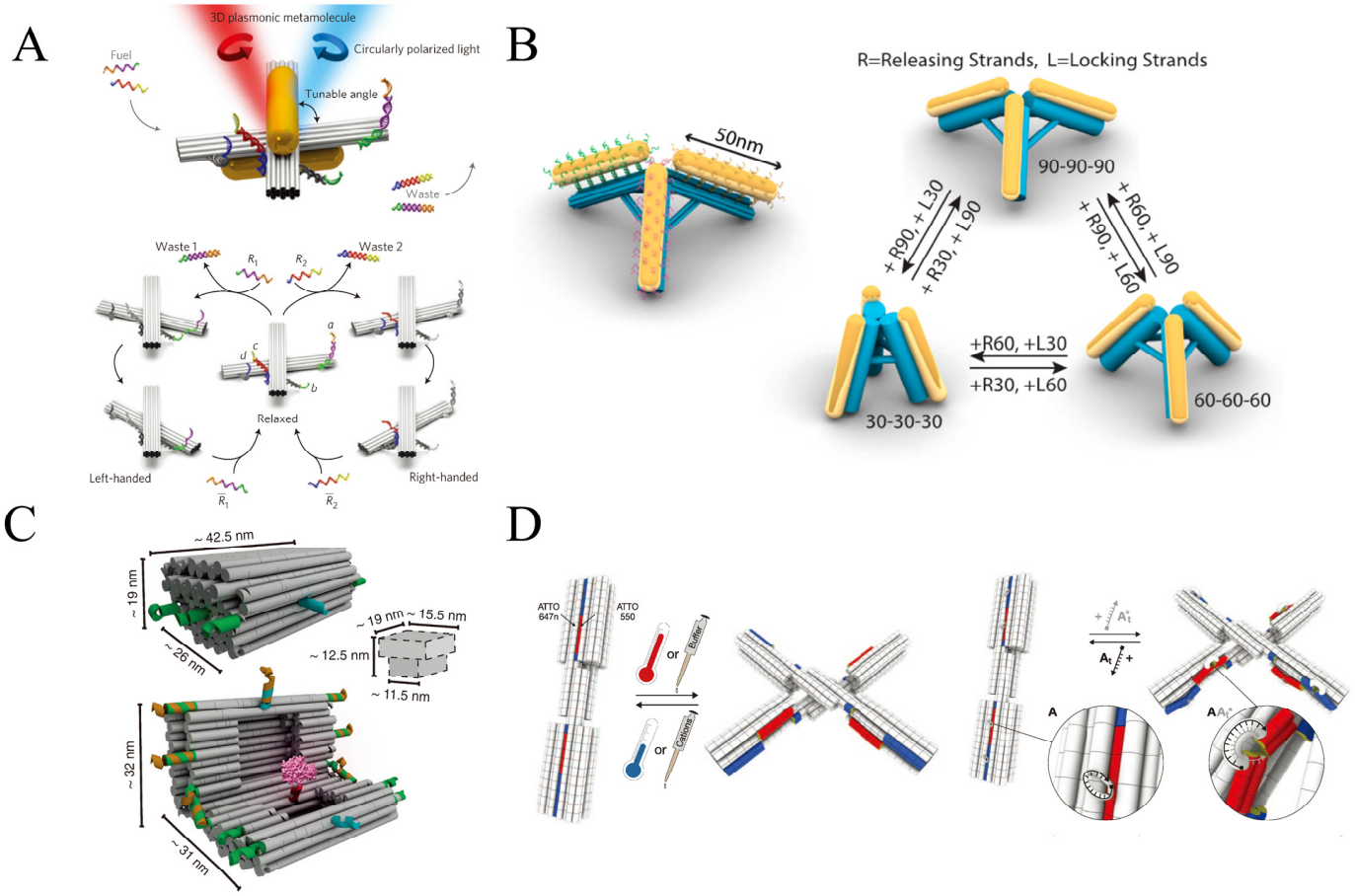

Figure 7. Shear motion nanodevices. (**A**) DNA locks and fuel strand-controlled reconfigurable 3D plasmonic metamolecules [12]. Copyright 2014, Springer Nature. (**B**) Use toehold-mediated strand displacement to adjust angles of DNA origami linking AuNP tripod [126]. Copyright 2017, American Chemical Society. (**C**) Toehold-mediated DNA strand displacement to Control Opening and Closing of DNA Vault (DV); DV is used to control the enzymatic reaction catalyzed by an electrolyte protease [127]. Copyright 2017, Springer Nature. (**D**) Shape-complementary DNA pliers can be reversibly reconfigured by cation concentration or temperature changes, along with a site-specific allosteric control mechanism. A^*_t is complementary to the single-stranded loops on the switch and features an additional nine-bases-long toehold motif. At is fully complementary to A^*_t and can be used to displace A^*_t again fromthe switch [130]. Copyright 2015, American Association for the Advancement of Science.

4.3. 360° Rotation

360° rotation is a common movement in life. Wheels, gears, and the rotor of an engine are all common rotating parts. In the second half of the 20th century, researchers discovered rotational mechanisms in nature, including flagella motors [131] and F1F0-ATPase [132–134].

The field of research focused on developing devices that utilize DNA nanostructures to mimic the behavior of macroscopic rotors is experiencing a significant proliferation of studies and advancements. In 2016, Ketterer et al. proposed a DNA origami system, which was composed of a rotor unit and two clamp elements that form an axle bearing (Figure 8A). The rotor is thermally driven inside the clamp dimer, and introducing six instead of two shape-complementary docking can make the rotor multistate switching on up to six dwell positions spaced. The rotor can rotate indefinitely through Brownian motion,

but the docking position cannot be precisely controlled [120]. Tomaru et al. proposed a DNA rotation system by adding four different sets of DNA strands and controlling the rotor to point in four different directions (0°, 90°, 180°, and −90°) through the reaction to strand displacement (Figure 8B). Further mentioned above are some 360° rotating devices with precise spatiotemporal control based on the drive or magnetic drive [134].

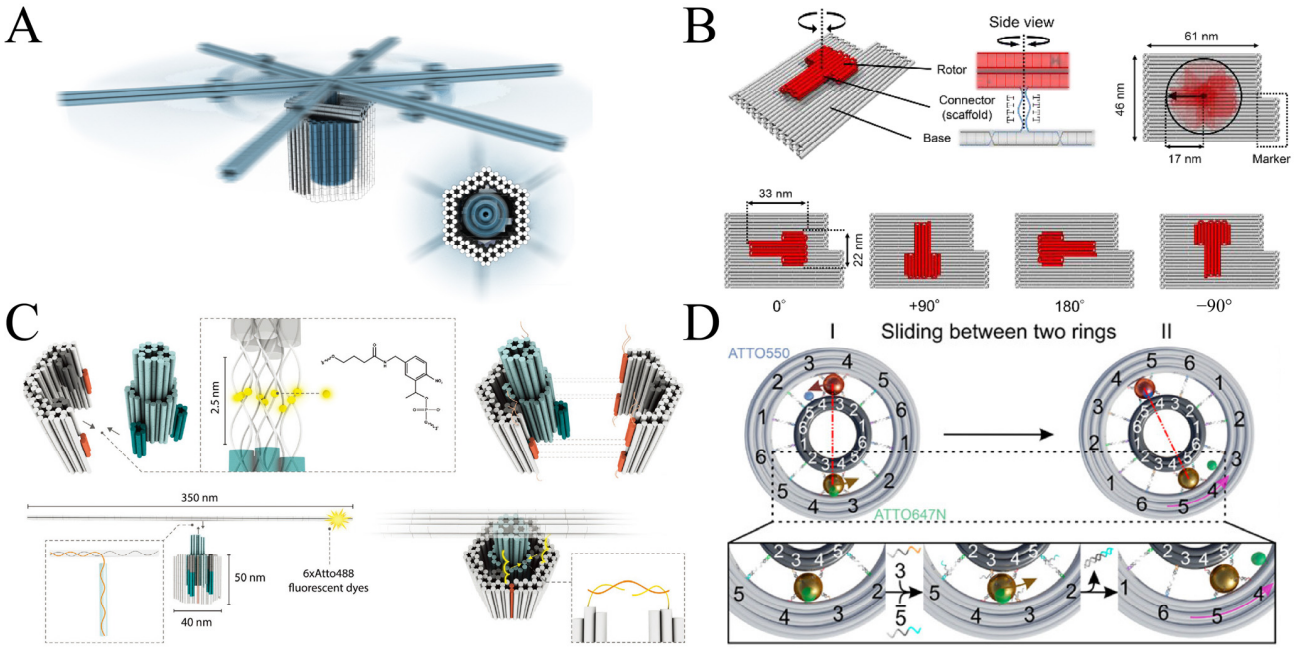

Figure 8. Nanodevices that rotate 360 degrees. (**A**) The spinning DNA rotor is driven by Brownian motion, the blue is the rotor unit and the gray is the clamp unit [120]. Copyright 2016, American Association for the Advancement of Science. (**B**) A DNA rotation device directed to four different orientations is controlled by strand displacement, Different colors represent different parts: base (gray), rotor (red) and connector (blue). Sequence of the single stranded connector has only thymine bases [134]. Copyright 2017. Royal Society of Chemistry. (**C**) DNA rotation device driven by fluid drive and Brownian motion [33]. Copyright 2020, John Wiley and Sons. (**D**) The DNA nanodevice mimicking the two-Cogwheel gear system consists of two origami rings and two gold nanoparticles. Two AuNPs as planet gears sliding in between the small ring (sun gear) and large ring (ring gear) in a planetary gearset nanodevice. Fluorophore ATTO550 (blue) is tethered on the small ring between foothold rows 4 and 5, while fluorophore ATTO647N (green) is attached to the large ring between foothold rows 3 and 4 [135]. Copyright 2022, American Chemical Society.

In addition to strand displacement [134,135], electromagnetic drive [10,92,95], and Brownian motion [120], other rotational driving mechanisms have been investigated as alternative methods by researchers in this field. Ahmadi et al. proposed a fluid-driven rotating device, and the researchers used single-molecule microscopy in a microfluidic chamber setup to analyze its Brownian and flow-driven rotational dynamics (Figure 8C). It is found that the rotor can switch between three states, and the maneuverability is increased at a moderate flow, but controllable rotation cannot be achieved [33].

Recently, Peil et al. proposed a DNA origami device that mimics the operation of a two-cogwheel gear system (Figure 8D). This system consists of a small origami ring, a large origami ring, and gold nanoparticles (AuNPs). The inner side of the larger ring, the outer side of the smaller ring, and the gold nanospheres have foothold strands that allow rotation via strand displacement reactions [135]. Kosuri et al. developed the origami-rotor-based imaging and tracking (ORBIT) technique, which tracks DNA rotation at the single-molecule level with a millisecond-level time resolution using fluorescently labeled DNA origami rotors. Researchers tracked DNA rotations caused by transcription by RNAP

and unwinding by the RecBCD complex, a helicase involved in DNA repair, using ORBIT. They described several activities involved in RecBCD-induced DNA unwinding, such as initiation, processive translocation, stopping, and backtracking. They also identified a starting mechanism involving reversible ATP-independent DNA unwinding and the activation of the RecB motor [10].

4.4. Complex Motion

Complex motion is a combination of rotation and translation. J. Urban et al. reported a plasmonic walker couple system (Figure 9A). The device is primarily composed of four parts, namely three AuNRs and an origami template. Among the three AuNRs, two AuNRs on the same plane can walk independently or are simultaneously driven by DNA hybridization, while the other AuNR is fixed. To resolve such dynamic walking with nanoscale steps well below the optical diffraction limit, the researchers use optical spectroscopy. Researchers have also demonstrated a correlation between the number of walkers and the system's optical response [49].

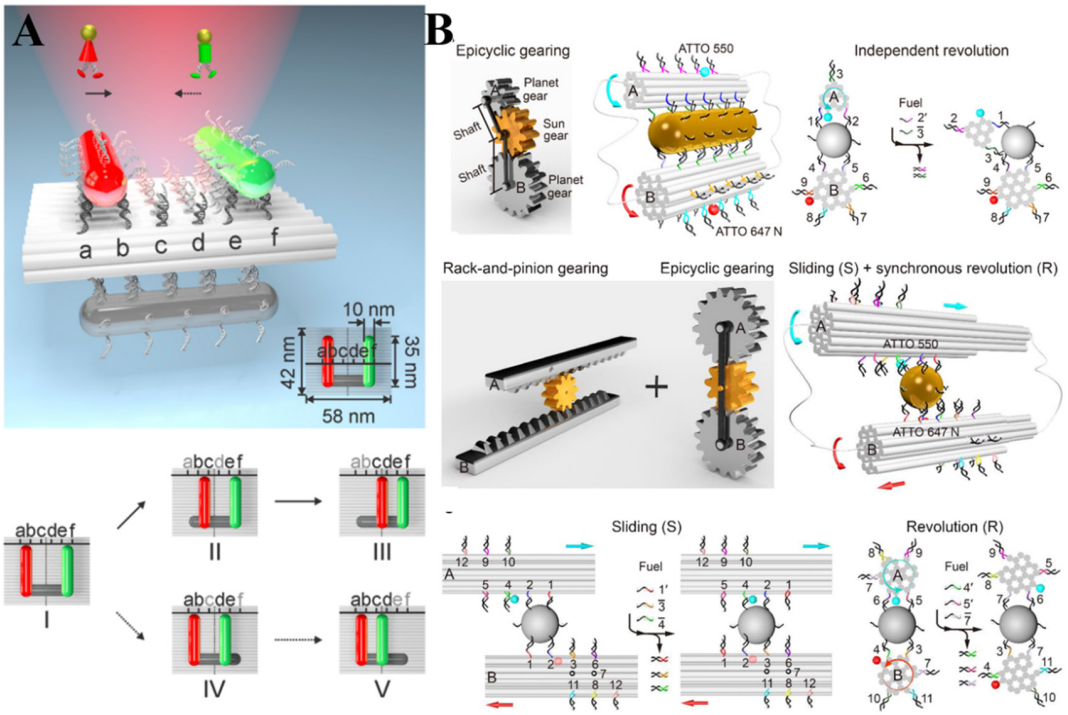

Figure 9. Nanodevices capable of complex movements. (**A**) A plasmonic walker-coupled system consisting of three AuNPs of DNA Origami plate, where red and green AuNPs are capable of movement, while gray AuNPs are stationary. The individual walkers (AuNPs) use toehold-mediated strand displacement processes that complete the step-by-step walk. In state I, the walkers are initially positioned symmetrically at the two ends of the stator. On the upper route, the green walker remains stationary while the red walker takes two consecutive steps, advancing to states II and III, respectively. On the lower route, the red walker pauses while the green walker performs two successive steps, progressing to states IV and V, respectively [49]. Copyright 2015, American Chemical Society. (**B**) DNA origami filaments (white), gold nanocrystals (golden yellow), and fluorophores (red or blue) form interlocking gears [136]. Copyright 2019, American Association for the Advancement of Science.

Many DNA nanodevices, mimicking macroscopic mechanical devices, are capable of performing complex movements. Zhan et al. used DNA origami filaments, gold nanocrystals and fluorophores to form interlocking gears (Figure 9B). These individual building blocks can execute independent, synchronous, or joint motion upon external inputs. From the side view, the DNA origami filaments in the epicyclic gearset were also correlated with

translation in addition to the rotation, while rate-and-pinion gearing involved both rotation and translation. Therefore, these two systems are complex movements [136]. Marras et al. assembled a DNA crank-slider using one DNA origami slider joint and three hinges that performed constrained linear and rotational motion. The slider is made up of two stiff parts that are folded tightly together and are only joined by a ssDNA scaffold to allow for linear motion. Thermally driven sliding of the joint unit along the origami tube and movement of the hinge arms are made possible by the thermal fluctuation of the flexible ssDNA scaffold connections [137].

5. Conclusions

Tremendous success in DNA self-assembly technology makes it possible to design and produce controllable dynamic DNA nanodevices. In recent decades, numerous DNA nanodevices with unique structures and functi , have been manufactured, which can conduct a variety of motions in response to specific stimuli. This review begins with a brief history of the development of DNA self-assembly, followed by a summary of two classical DNA self-assembly techniques for the construction of dynamic DNA nanostructures. The mechanisms of the dynamic behavior of DNA nanodevices are discussed regarding different types of driving energies, such as the strand displacement reaction, light, electric and magnetic fields, pH, and ion concentration. Finally, we systematically classify the reported forms of nanodevice motion. These dynamic DNA nanodevices have shown significant potential in the biomedical field, which could be used for drug delivery, interrogating cellular progress, or biosensing.

However, several crucial challenges need to be addressed before future practical applications [39,42,138–141]. First, the biological applications of DNA nanomaterials are still at a relatively early stage of exploration. The biodistribution, pharmacokinetics, and biosafety of DNA nanomaterials still require a great effort to be comprehensively investigated. Because DNA-based nanomaterials are very sensitive to nuclease, they are highly susceptible to degradation in serum [142]. Unmodified DNA nanoparticles exhibit a limited lifespan of merely a few minutes after intravenous injection in mice [143,144]. To solve this problem, researchers have explored many methods to stabilize DNA structures in a biological environment, including lipid encapsulation [143], incubation and coating with intercalators [145], proteins [146], or cationic oligo- or polymers [144,147,148], PEGylation [149], combinations thereof, and minor groove binders [150]. Notably, the key point to consider when choosing these protection strategies is the ability to maintain the responsive allosteric properties of dynamic DNA nanostructures in physiological environments [150]. Furthermore, there is a need for further exploration of the mechanisms involved in the internalization, transportation, and dynamics of DNA nanodevices [90].

Second, the kinetics of DNA self-assembly is another vital parameter to research for the controlled manipulation of DNA nanostructures. DNA self-assembly is a delicate operation, and every step in the process, from the design of the molecular strand to the annealing process, affects the outcome of the assembly. For example, the difference in the force yielded by ssDNA and dsDNA under tension closely relates to their length, base sequence periodicity, and geometric structure. The currently reported DNA nanodevices were normally studied in pure solutions, which only can perform simple inputs. However, for multi-response dynamic DNA nanomachines, there are various competitive relationships, such as toehold-mediated strand displacement, key–lock system, the ligand and complementary strands competitively bonding to the aptamer, etc. However, nowadays, scientists focus more on the final structure of DNA assembly and less on the kinetics of assembly and its influencing factors. Therefore, it is necessary to conduct an in-depth study of the mechanical properties of DNA structures by means of computer simulations.

Another considerable challenge for the application is the DNA production cost. Hopefully, recent advancements in synthesis and biotechnological methods have reduced its price, including intracellular production, rolling circle amplification (RCA), asymmetric PCR, and fermentation [151]. Based on researchers' statistics, the raw material cost for

manufacturing 1 mg of DNA origami using conventional methods is nearly £200 [152]. Praetorius introduced a biotechnology technique that can lower the cost of DNA origami to €0.18 per milligram (£0.154 with the exchange rate as of 29 July 2023), incorporating not only the material expenses but also the labor and management costs. This approach is relatively more suitable for large-scale production [153].

DNA nanodevices are assembled using a 'bottom-up' self-assembly approach, utilizing DNA molecules that can be further modified with biomolecules or nanoparticles to achieve various functionalities. Due to their stability and biosafety, DNA nanodevices are highly suitable for diverse applications, including drug delivery, targeted therapies, biosensing, and disease diagnosis. The exceptional potential and rapid advancement of DNA nanodevices are expected to have a profound impact on the fields of synthetic biology, medicine, and diagnostics, playing an indispensable and distinct role.

Author Contributions: Writing—original draft preparation, Q.F. and L.Y.; writing—review and editing, Q.F. and J.C.; funding acquisition, Q.F. and J.C. All authors have read and agreed to the published version of the manuscript.

Funding: This work was supported by the National Nature Science Foundation of China (21922408 and 22274081), the Natural Science Foundation of Jiangsu Province (No. BK20220401), the Natural Science Foundation of Jiangsu Province-Major Project (BK20212012), the Project of State Key Laboratory of Organic Electronics and Information Displays (No. GDX2022010006 and No. GZR2022010029), and the Natural Science Research Start-up Foundation of Recruiting Talents of Nanjing University of Posts and Telecommunications (No. NY221132).

Data Availability Statement: Data available in a publicly accessible repository and cited in accordance with journal guidelines.

Conflicts of Interest: The authors declare no conflict of interest.

References

1. Ramezani, H.; Dietz, H. Building machines with DNA molecules. *Nat. Rev. Genet.* **2020**, *21*, 5–26. [CrossRef]
2. Smith, S.B.; Cui, Y.; Bustamante, C. Overstretching B-DNA: The elastic response of individual double-stranded and single-stranded DNA molecules. *Science* **1996**, *271*, 795–799. [CrossRef]
3. Gore, J.; Bryant, Z.; Nöllmann, M.; Le, M.U.; Cozzarelli, N.R.; Bustamante, C. DNA overwinds when stretched. *Nature* **2006**, *442*, 836–839. [CrossRef] [PubMed]
4. Tian, Y.; Wang, T.; Liu, W.; Xin, H.L.; Li, H.; Ke, Y.; Shih, W.M.; Gang, O. Prescribed nanoparticle cluster architectures and low-dimensional arrays built using octahedral DNA origami frames. *Nat. Nanotechnol.* **2015**, *10*, 637–644. [CrossRef] [PubMed]
5. Liu, J.; Jing, X.; Liu, M.; Li, F.; Li, M.; Li, Q.; Shi, J.; Li, J.; Wang, L.; Mao, X. Mechano-fluorescence actuation in single synaptic vesicles with a DNA framework nanomachine. *Sci. Robot.* **2022**, *7*, eabq5151. [CrossRef] [PubMed]
6. Zhou, Y.; Dong, J.; Zhou, C.; Wang, Q. Finite assembly of three-dimensional DNA hierarchical nanoarchitectures through orthogonal and directional bonding. *Angew. Chem. Int. Ed. Engl.* **2022**, *61*, e202116416.
7. Shen, Q.; Xiong, Q.; Zhou, K.; Feng, Q.; Liu, L.; Tian, T.; Wu, C.; Xiong, Y.; Melia, T.J.; Lusk, C.P.; et al. Functionalized DNA-origami-protein nanopores generate large transmembrane channels with programmable size-selectivity. *J. Am. Chem. Soc.* **2022**, *145*, 1292–1300. [CrossRef] [PubMed]
8. Manuguri, S.; Nguyen, M.-K.; Loo, J.; Natarajan, A.K.; Kuzyk, A. Advancing the utility of DNA origami technique through enhanced stability of DNA-origami-based assemblies. *Bioconjug. Chem.* **2022**, *34*, 6–17. [CrossRef]
9. Knappe, G.A.; Wamhoff, E.-C.; Bathe, M. Functionalizing DNA origami to investigate and interact with biological systems. *Nat. Rev. Mater.* **2022**, *8*, 123–138. [CrossRef]
10. Kosuri, P.; Altheimer, B.D.; Dai, M.; Yin, P.; Zhuang, X. Rotation tracking of genome-processing enzymes using DNA origami rotors. *Nature* **2019**, *572*, 136–140. [CrossRef]
11. Choi, Y.; Choi, H.; Lee, A.C.; Lee, H.; Kwon, S. A reconfigurable DNA accordion rack. *Angew. Chem. Int. Ed. Engl.* **2018**, *57*, 2811–2815. [CrossRef] [PubMed]
12. Kuzyk, A.; Schreiber, R.; Zhang, H.; Govorov, A.O.; Liedl, T.; Liu, N. Reconfigurable 3D plasmonic metamolecules. *Nat. Mater.* **2014**, *13*, 862–866. [CrossRef] [PubMed]
13. Zhang, Y.; Wang, F.; Chao, J.; Xie, M.; Liu, H.; Pan, M.; Kopperger, E.; Liu, X.; Li, Q.; Shi, J.; et al. DNA origami cryptography for secure communication. *Nat. Commun.* **2019**, *10*, 5469. [CrossRef] [PubMed]
14. Pan, K.; Kim, D.-N.; Zhang, F.; Adendorff, M.R.; Yan, H.; Bathe, M. Lattice-free prediction of three-dimensional structure of programmed DNA assemblies. *Nat. Commun.* **2014**, *5*, 5578. [CrossRef] [PubMed]

15. Poppleton, E.; Bohlin, J.; Matthies, M.; Sharma, S.; Zhang, F.; Šulc, P. Design, optimization and analysis of large DNA and RNA nanostructures through interactive visualization, editing and molecular simulation. *Nucleic Acids Res.* **2020**, *48*, e72. [CrossRef]
16. Reshetnikov, R.V.; Stolyarova, A.V.; Zalevsky, A.O.; Panteleev, D.Y.; Pavlova, G.V.; Klinov, D.V.; Golovin, A.V.; Protopopova, A.D. A coarse-grained model for DNA origami. *Nucleic Acids Res.* **2018**, *46*, 1102–1112. [CrossRef] [PubMed]
17. Dey, S.; Fan, C.; Gothelf, K.V.; Li, J.; Lin, C.; Liu, L.; Liu, N.; Nijenhuis, M.A.; Saccà, B.; Simmel, F.C. DNA origami. *Nat. Rev. Methods Primers* **2021**, *1*, 13. [CrossRef]
18. Seeman, N.C. DNA in a material world. *Nature* **2003**, *421*, 427–431. [CrossRef]
19. Burns, J.R.; Lamarre, B.; Pyne, A.L.B.; Noble, J.E.; Ryadnov, M.G. DNA origami inside-out viruses. *ACS Synth. Biol.* **2018**, *7*, 767–773. [CrossRef]
20. Keller, A.; Linko, V. Challenges and perspectives of DNA nanostructures in biomedicine. *Angew. Chem. Int. Ed. Engl.* **2020**, *59*, 15818–15833. [CrossRef]
21. Rajwar, A.; Kharbanda, S.; Chandrasekaran, A.R.; Gupta, S.; Bhatia, D. Designer, Programmable 3D DNA nanodevices to probe biological systems. *ACS Appl. Bio Mater.* **2020**, *3*, 7265–7277. [CrossRef]
22. Mela, I.; Vallejo-Ramirez, P.P.; Makarchuk, S.; Christie, G.; Bailey, D.; Henderson, R.M.; Sugiyama, H.; Endo, M.; Kaminski, C.F. DNA nanostructures for targeted antimicrobial delivery. *Angew. Chem. Int. Ed. Engl.* **2020**, *59*, 12698–12702. [CrossRef] [PubMed]
23. Watson, J.D.; Crick, F.H. Molecular structure of nucleic acids: A structure for deoxyribose nucleic acid. *Nature* **1953**, *171*, 737–738. [CrossRef]
24. Seeman, N.C. Nucleic acid junctions and lattices. *J. Theor. Biol.* **1982**, *99*, 237–247. [CrossRef] [PubMed]
25. Kallenbach, N.R.; Ma, R.-I.; Seeman, N.C. An immobile nucleic acid junction constructed from oligonucleotides. *Nature* **1983**, *305*, 829–831. [CrossRef]
26. Shih, W.M.; Quispe, J.D.; Joyce, G.F. A 1.7-kilobase single-stranded DNA that folds into a nanoscale octahedron. *Nature* **2004**, *427*, 618–621. [CrossRef]
27. Rothemund, P.W. Folding DNA to create nanoscale shapes and patterns. *Nature* **2006**, *440*, 297–302. [CrossRef]
28. Andersen, E.S.; Dong, M.; Nielsen, M.M.; Jahn, K.; Lind-Thomsen, A.; Mamdouh, W.; Gothelf, K.V.; Besenbacher, F.; Kjems, J. DNA origami design of dolphin-shaped structures with flexible tails. *ACS Nano* **2008**, *2*, 1213–1218. [CrossRef]
29. Tikhomirov, G.; Petersen, P.; Qian, L. Triangular DNA Origami Tilings. *J. Am. Chem. Soc.* **2018**, *140*, 17361–17364. [CrossRef]
30. Rajendran, A.; Endo, M.; Katsuda, Y.; Hidaka, K.; Sugiyama, H. Programmed two-dimensional self-assembly of multiple DNA origami jigsaw pieces. *ACS Nano* **2011**, *5*, 665–671. [CrossRef]
31. Douglas, S.M.; Dietz, H.; Liedl, T.; Högberg, B.; Graf, F.; Shih, W.M. Self-assembly of DNA into nanoscale three-dimensional shapes. *Nature* **2009**, *459*, 414–418. [CrossRef] [PubMed]
32. Pumm, A.K.; Engelen, W.; Kopperger, E.; Isensee, J.; Vogt, M.; Kozina, V.; Kube, M.; Honemann, M.N.; Bertosin, E.; Langecker, M.; et al. A DNA origami rotary ratchet motor. *Nature* **2022**, *607*, 492–498. [CrossRef] [PubMed]
33. Ahmadi, Y.; Nord, A.L.; Wilson, A.J.; Hutter, C.; Schroeder, F.; Beeby, M.; Barisic, I. The brownian and flow-driven rotational dynamics of a multicomponent DNA origami-based rotor. *Small* **2020**, *16*, e2001855. [CrossRef]
34. Li, H.; Gao, J.; Cao, L.; Xie, X.; Fan, J.; Wang, H.; Wang, H.H.; Nie, Z. A DNA molecular robot that autonomously walks on the cell membrane to drive cell motility. *Angew. Chem. Int. Ed. Engl.* **2021**, *60*, 26087–26095. [CrossRef]
35. Thubagere, A.J.; Li, W.; Johnson, R.F.; Chen, Z.; Doroudi, S.; Lee, Y.L.; Izatt, G.; Wittman, S.; Srinivas, N.; Woods, D.; et al. A cargo-sorting DNA robot. *Science* **2017**, *357*, eaan6558. [CrossRef] [PubMed]
36. Lund, K.; Manzo, A.J.; Dabby, N.; Michelotti, N.; Johnson-Buck, A.; Nangreave, J.; Taylor, S.; Pei, R.; Stojanovic, M.N.; Walter, N.G.; et al. Molecular robots guided by prescriptive landscapes. *Nature* **2010**, *465*, 206–210. [CrossRef]
37. Kwon, P.S.; Ren, S.; Kwon, S.J.; Kizer, M.E.; Kuo, L.; Xie, M.; Zhu, D.; Zhou, F.; Zhang, F.; Kim, D.; et al. Designer DNA architecture offers precise and multivalent spatial pattern-recognition for viral sensing and inhibition. *Nat. Chem.* **2020**, *12*, 26–35. [CrossRef] [PubMed]
38. Ma, W.; Yan, L.; He, X.; Qing, T.; Lei, Y.; Qiao, Z.; He, D.; Huang, K.; Wang, K. Hairpin-contained i-motif based fluorescent ratiometric probe for high-resolution and sensitive response of small pH variations. *Anal. Chem.* **2018**, *90*, 1889–1896. [CrossRef]
39. Leung, K.; Chakraborty, K.; Saminathan, A.; Krishnan, Y. A DNA nanomachine chemically resolves lysosomes in live cells. *Nat. Nanotechnol.* **2019**, *14*, 176–183. [CrossRef]
40. Zhuang, X.; Ma, X.; Xue, X.; Jiang, Q.; Song, L.; Dai, L.; Zhang, C.; Jin, S.; Yang, K.; Ding, B.; et al. A photosensitizer-loaded DNA origami nanosystem for photodynamic therapy. *ACS Nano* **2016**, *10*, 3486–3495. [CrossRef]
41. Wiraja, C.; Zhu, Y.; Lio, D.C.S.; Yeo, D.C.; Xie, M.; Fang, W.; Li, Q.; Zheng, M.; Van Steensel, M.; Wang, L. Framework nucleic acids as programmable carrier for transdermal drug delivery. *Nat. Commun.* **2019**, *10*, 1147. [CrossRef] [PubMed]
42. Li, S.; Jiang, Q.; Liu, S.; Zhang, Y.; Tian, Y.; Song, C.; Wang, J.; Zou, Y.; Anderson, G.J.; Han, J.-Y. A DNA nanorobot functions as a cancer therapeutic in response to a molecular trigger in vivo. *Nat. Biotechnol.* **2018**, *36*, 258–264. [CrossRef] [PubMed]
43. Zhao, Z.; Fu, J.; Dhakal, S.; Johnson-Buck, A.; Liu, M.; Zhang, T.; Woodbury, N.W.; Liu, Y.; Walter, N.G.; Yan, H. Nanocaged enzymes with enhanced catalytic activity and increased stability against protease digestion. *Nat. Commun.* **2016**, *7*, 10619. [CrossRef] [PubMed]
44. Fu, Y.; Zeng, D.; Chao, J.; Jin, Y.; Zhang, Z.; Liu, H.; Li, D.; Ma, H.; Huang, Q.; Gothelf, K.V.; et al. Single-step rapid assembly of DNA origami nanostructures for addressable nanoscale bioreactors. *J. Am. Chem. Soc.* **2013**, *135*, 696–702. [CrossRef]

45. Liu, W.; Tagawa, M.; Xin, H.L.; Wang, T.; Emamy, H.; Li, H.; Yager, K.G.; Starr, F.W.; Tkachenko, A.V.; Gang, O. Diamond family of nanoparticle superlattices. *Science* **2016**, *351*, 582–586. [CrossRef]
46. Tian, Y.; Zhang, Y.; Wang, T.; Xin, H.L.; Li, H.; Gang, O. Lattice engineering through nanoparticle–DNA frameworks. *Nat. Mater.* **2016**, *15*, 654–661. [CrossRef]
47. Douglas, S.M.; Bachelet, I.; Church, G.M. A logic-gated nanorobot for targeted transport of molecular payloads. *Science* **2012**, *335*, 831–834. [CrossRef]
48. Prokup, A.; Hemphill, J.; Deiters, A. DNA computation: A photochemically controlled AND gate. *J. Am. Chem. Soc.* **2012**, *134*, 3810–3815. [CrossRef]
49. Urban, M.J.; Zhou, C.; Duan, X.; Liu, N. Optically resolving the dynamic walking of a plasmonic walker couple. *Nano Lett.* **2015**, *15*, 8392–8396. [CrossRef]
50. Lan, X.; Liu, T.; Wang, Z.; Govorov, A.O.; Yan, H.; Liu, Y. DNA-guided plasmonic helix with switchable chirality. *J. Am. Chem. Soc.* **2018**, *140*, 11763–11770. [CrossRef]
51. Zhou, C.; Xin, L.; Duan, X.; Urban, M.J.; Liu, N. Dynamic plasmonic system that responds to thermal and aptamer-target Regulations. *Nano Lett.* **2018**, *18*, 7395–7399. [CrossRef] [PubMed]
52. Ijas, H.; Hakaste, I.; Shen, B.; Kostiainen, M.A.; Linko, V. Reconfigurable DNA origami nanocapsule for pH-controlled encapsulation and display of cargo. *ACS Nano* **2019**, *13*, 5959–5967. [CrossRef] [PubMed]
53. Jiang, Q.; Liu, S.; Liu, J.; Wang, Z.G.; Ding, B. Rationally designed DNA-origami nanomaterials for drug delivery in vivo. *Adv. Mater.* **2019**, *31*, e1804785. [CrossRef]
54. Shen, C.; Lan, X.; Lu, X.; Ni, W.; Wang, Q. Tuning the structural asymmetries of three-dimensional gold nanorod assemblies. *Chem. Commun.* **2015**, *51*, 13627–13629. [CrossRef]
55. Li, M.; Yang, G.; Zheng, Y.; Lv, J.; Zhou, W.; Zhang, H.; You, F.; Wu, C.; Yang, H.; Liu, Y. NIR/pH-triggered aptamer-functionalized DNA origami nanovehicle for imaging-guided chemo-phototherapy. *J. Nanobiotechnol.* **2023**, *21*, 186. [CrossRef] [PubMed]
56. Douglas, S.M.; Marblestone, A.H.; Teerapittayanon, S.; Vazquez, A.; Church, G.M.; Shih, W.M. Rapid prototyping of 3D DNA-origami shapes with caDNAno. *Nucleic Acids Res.* **2009**, *37*, 5001–5006. [CrossRef]
57. Benson, E.; Mohammed, A.; Gardell, J.; Masich, S.; Czeizler, E.; Orponen, P.; Högberg, B. DNA rendering of polyhedral meshes at the nanoscale. *Nature* **2015**, *523*, 441–444. [CrossRef]
58. Jun, H.; Wang, X.; Bricker, W.P.; Jackson, S.; Bathe, M. Rapid prototyping of arbitrary 2D and 3D wireframe DNA origami. *Nucleic Acids Res.* **2021**, *49*, 10265–10274. [CrossRef]
59. Yoo, J.; Aksimentiev, A. In situ structure and dynamics of DNA origami determined through molecular dynamics simulations. *Proc. Natl. Acad. Sci. USA* **2013**, *110*, 20099–20104. [CrossRef]
60. Göpfrich, K.; Li, C.-Y.; Ricci, M.; Bhamidimarri, S.P.; Yoo, J.; Gyenes, B.; Ohmann, A.; Winterhalter, M.; Aksimentiev, A.; Keyser, U.F. Large-conductance transmembrane porin made from DNA origami. *ACS Nano* **2016**, *10*, 8207–8214. [CrossRef]
61. Doye, J.P.; Ouldridge, T.E.; Louis, A.A.; Romano, F.; Sulc, P.; Matek, C.; Snodin, B.E.; Rovigatti, L.; Schreck, J.S.; Harrison, R.M.; et al. Coarse-graining DNA for simulations of DNA nanotechnology. *Phys. Chem. Chem. Phys.* **2013**, *15*, 20395–20414. [CrossRef] [PubMed]
62. Snodin, B.E.; Randisi, F.; Mosayebi, M.; Šulc, P.; Schreck, J.S.; Romano, F.; Ouldridge, T.E.; Tsukanov, R.; Nir, E.; Louis, A.A. Introducing improved structural properties and salt dependence into a coarse-grained model of DNA. *J. Chem. Phys.* **2015**, *142*, 234901. [CrossRef] [PubMed]
63. Orponen, P. Design methods for 3D wireframe DNA nanostructures. *Nat. Comput.* **2018**, *17*, 147–160. [CrossRef]
64. Han, D. Design of wireframe DNA nanostructures-DNA gridiron. *Methods Mol. Biol.* **2017**, *1500*, 27–40.
65. Simmel, S.S.; Nickels, P.C.; Liedl, T. Wireframe and tensegrity DNA nanostructures. *Acc. Chem. Res.* **2014**, *47*, 1691–1699. [CrossRef]
66. Dong, Y.; Yao, C.; Zhu, Y.; Yang, L.; Luo, D.; Yang, D. DNA functional materials assembled from branched DNA: Design, synthesis, and applications. *Chem. Rev.* **2020**, *120*, 9420–9481. [CrossRef]
67. Yang, X.; Vologodskii, A.V.; Liu, B.; Kemper, B.; Seeman, N.C. Torsional control of double-stranded DNA branch migration. *Biopolymers* **1998**, *45*, 69–83. [CrossRef]
68. Simmel, F.C.; Yurke, B.; Singh, H.R. Principles and applications of nucleic acid strand displacement reactions. *Chem. Rev.* **2019**, *119*, 6326–6369. [CrossRef]
69. Yurke, B.; Turberfield, A.J.; Mills, A.P., Jr.; Simmel, F.C.; Neumann, J.L. A DNA-fuelled molecular machine made of DNA. *Nature* **2000**, *406*, 605–608. [CrossRef]
70. Ke, Y.; Meyer, T.; Shih, W.M.; Bellot, G. Regulation at a distance of biomolecular interactions using a DNA origami nanoactuator. *Nat. Commun.* **2016**, *7*, 10935. [CrossRef]
71. Chao, J.; Wang, J.; Wang, F.; Ouyang, X.; Kopperger, E.; Liu, H.; Li, Q.; Shi, J.; Wang, L.; Hu, J.; et al. Solving mazes with single-molecule DNA navigators. *Nat. Mater.* **2019**, *18*, 273–279. [CrossRef] [PubMed]
72. Sherman, W.B.; Seeman, N.C. A precisely controlled DNA biped walking device. *Nano Lett.* **2004**, *4*, 1203–1207. [CrossRef]
73. Shin, J.S.; Pierce, N.A. A synthetic DNA walker for molecular transport. *J. Am. Chem. Soc.* **2004**, *126*, 10834–10835. [CrossRef] [PubMed]
74. Wang, C.; O'Hagan, M.P.; Li, Z.; Zhang, J.; Ma, X.; Tian, H.; Willner, I. Photoresponsive DNA materials and their applications. *Chem. Soc. Rev.* **2022**, *51*, 720–760. [CrossRef] [PubMed]

75. Ryssy, J.; Natarajan, A.K.; Wang, J.; Lehtonen, A.J.; Nguyen, M.K.; Klajn, R.; Kuzyk, A. Light-responsive dynamic DNA-Origami-based plasmonic assemblies. *Angew. Chem. Int. Ed. Engl.* **2021**, *60*, 5859–5863. [CrossRef]
76. Waldeck, D.H. Photoisomerization dynamics of stilbenes. *Chem. Rev.* **1991**, *91*, 415–436. [CrossRef]
77. Beharry, A.A.; Woolley, G.A. Azobenzene photoswitches for biomolecules. *Chem. Soc. Rev.* **2011**, *40*, 4422–4437. [CrossRef]
78. Bandara, H.M.; Burdette, S.C. Photoisomerization in different classes of azobenzene. *Chem. Soc. Rev.* **2012**, *41*, 1809–1825. [CrossRef]
79. Berkovic, G.; Krongauz, V.; Weiss, V. Spiropyrans and spirooxazines for memories and switches. *Chem. Rev.* **2000**, *100*, 1741–1754. [CrossRef]
80. Lukyanov, B.; Lukyanova, M. Spiropyrans: Synthesis, properties, and application. *Chem. Heterocycl. Compd.* **2005**, *41*, 281–311. [CrossRef]
81. Liang, X.; Nishioka, H.; Takenaka, N.; Asanuma, H. A DNA nanomachine powered by light irradiation. *ChemBioChem* **2008**, *9*, 702–705. [CrossRef] [PubMed]
82. Lohmann, F.; Ackermann, D.; Famulok, M. Reversible light switch for macrocycle mobility in a DNA rotaxane. *J. Am. Chem. Soc.* **2012**, *134*, 11884–11887. [CrossRef] [PubMed]
83. Wang, J.; Yue, L.; Li, Z.; Zhang, J.; Tian, H.; Willner, I. Active generation of nanoholes in DNA origami scaffolds for programmed catalysis in nanocavities. *Nat. Commun.* **2019**, *10*, 4963. [CrossRef] [PubMed]
84. Yang, Y.; Goetzfried, M.A.; Hidaka, K.; You, M.; Tan, W.; Sugiyama, H.; Endo, M. Direct visualization of walking motions of photocontrolled nanomachine on the DNA nanostructure. *Nano Lett.* **2015**, *15*, 6672–6676. [CrossRef]
85. Yang, Y.; Endo, M.; Hidaka, K.; Sugiyama, H. Photo-controllable DNA origami nanostructures assembling into predesigned multiorientational patterns. *J. Am. Chem. Soc.* **2012**, *134*, 20645–20653. [CrossRef]
86. Willner, E.M.; Kamada, Y.; Suzuki, Y.; Emura, T.; Hidaka, K.; Dietz, H.; Sugiyama, H.; Endo, M. Single-molecule observation of the photoregulated conformational dynamics of DNA origami nanoscissors. *Angew. Chem. Int. Ed. Engl.* **2017**, *56*, 15324–15328. [CrossRef]
87. Kandatsu, D.; Cervantes-Salguero, K.; Kawamata, I.; Hamada, S.; Nomura, S.i.M.; Fujimoto, K.; Murata, S. Reversible gel–sol transition of a photo-responsive DNA gel. *ChemBioChem* **2016**, *17*, 1118–1121. [CrossRef]
88. Anderson, R.R.; Parrish, J.A. The optics of human skin. *J. Investig. Dermatol.* **1981**, *77*, 13–19. [CrossRef]
89. Samanta, S.; Beharry, A.A.; Sadovski, O.; McCormick, T.M.; Babalhavaeji, A.; Tropepe, V.; Woolley, G.A. Photoswitching azo compounds in vivo with red light. *J. Am. Chem. Soc.* **2013**, *135*, 9777–9784. [CrossRef]
90. Hu, Y.; Wang, Y.; Yan, J.; Wen, N.; Xiong, H.; Cai, S.; He, Q.; Peng, D.; Liu, Z.; Liu, Y. Dynamic DNA assemblies in biomedical applications. *Adv. Sci.* **2020**, *7*, 2000557. [CrossRef]
91. Nummelin, S.; Shen, B.; Piskunen, P.; Liu, Q.; Kostiainen, M.A.; Linko, V. Robotic DNA nanostructures. *ACS Synth. Biol.* **2020**, *9*, 1923–1940. [CrossRef] [PubMed]
92. Kopperger, E.; List, J.; Madhira, S.; Rothfischer, F.; Lamb, D.C.; Simmel, F.C. A self-assembled nanoscale robotic arm controlled by electric fields. *Science* **2018**, *359*, 296–301. [CrossRef] [PubMed]
93. Liu, S.; Jiang, Q.; Wang, Y.; Ding, B. Biomedical applications of DNA-based molecular devices. *Adv. Healthc. Mater.* **2019**, *8*, e1801658. [CrossRef] [PubMed]
94. Stommer, P.; Kiefer, H.; Kopperger, E.; Honemann, M.N.; Kube, M.; Simmel, F.C.; Netz, R.R.; Dietz, H. A synthetic tubular molecular transport system. *Nat. Commun.* **2021**, *12*, 4393. [CrossRef] [PubMed]
95. Lauback, S.; Mattioli, K.R.; Marras, A.E.; Armstrong, M.; Rudibaugh, T.P.; Sooryakumar, R.; Castro, C.E. Real-time magnetic actuation of DNA nanodevices via modular integration with stiff micro-levers. *Nat. Commun.* **2018**, *9*, 1446. [CrossRef]
96. Nilsson, C.; Kågedal, K.; Johansson, U.; Öllinger, K. Analysis of cytosolic and lysosomal pH in apoptotic cells by flow cytometry. *Methods Cell Sci.* **2004**, *25*, 185–194. [CrossRef]
97. Wu, N.; Willner, I. pH-Stimulated reconfiguration and structural isomerization of origami dimer and trimer systems. *Nano Lett.* **2016**, *16*, 6650–6655. [CrossRef]
98. Gehring, K.; Leroy, J.L.; Gueron, M. A tetrameric DNA structure with protonated cytosine.cytosine base pairs. *Nature* **1993**, *363*, 561–565. [CrossRef]
99. Nonin, S.; Leroy, J.L. Structure and conversion kinetics of a bi-stable DNA i-motif: Broken symmetry in the [d(5mCCTCC)]4 tetramer. *J. Mol. Biol.* **1996**, *261*, 399–414. [CrossRef]
100. Collin, D.; Gehring, K. Stability of chimeric DNA/RNA cytosine tetrads: Implications for i-motif formation by RNA. *J. Am. Chem. Soc.* **1998**, *120*, 4069–4072. [CrossRef]
101. Hu, Y.; Cecconello, A.; Idili, A.; Ricci, F.; Willner, I. Triplex DNA nanostructures: From basic properties to applications. *Angew. Chem. Int. Ed. Engl.* **2017**, *56*, 15210–15233. [CrossRef]
102. Modi, S.; G., S.M.; Goswami, D.; Gupta, G.D.; Mayor, S.; Krishnan, Y. A DNA nanomachine that maps spatial and temporal pH changes inside living cells. *Nat. Nanotechnol.* **2009**, *4*, 325–330. [CrossRef]
103. Surana, S.; Bhat, J.M.; Koushika, S.P.; Krishnan, Y. An autonomous DNA nanomachine maps spatiotemporal pH changes in a multicellular living organism. *Nat. Commun.* **2011**, *2*, 340. [CrossRef]
104. Marras, A.E.; Shi, Z.; Lindell, M.G., 3rd; Patton, R.A.; Huang, C.M.; Zhou, L.; Su, H.J.; Arya, G.; Castro, C.E. Cation-activated avidity for rapid reconfiguration of DNA nanodevices. *ACS Nano* **2018**, *12*, 9484–9494. [CrossRef]

105. Patel, D.J.; Phan, A.T.; Kuryavyi, V. Human telomere, oncogenic promoter and 5′-UTR G-quadruplexes: Diverse higher order DNA and RNA targets for cancer therapeutics. *Nucleic Acids Res.* **2007**, *35*, 7429–7455. [CrossRef]
106. Neidle, S.; Parkinson, G.N. The structure of telomeric DNA. *Curr. Opin. Struct. Biol.* **2003**, *13*, 275–283. [CrossRef]
107. Smirnov, I.; Shafer, R.H. Lead is unusually effective in sequence-specific folding of DNA. *J. Mol. Biol.* **2000**, *296*, 1–5. [CrossRef] [PubMed]
108. Clever, G.H.; Soltl, Y.; Burks, H.; Spahl, W.; Carell, T. Metal-salen-base-pair complexes inside DNA: Complexation overrides sequence information. *Chemistry* **2006**, *12*, 8708–8718. [CrossRef] [PubMed]
109. Wojciechowski, F.; Leumann, C.J. Alternative DNA base-pairs: From efforts to expand the genetic code to potential material applications. *Chem. Soc. Rev.* **2011**, *40*, 5669–5679. [CrossRef] [PubMed]
110. Takezawa, Y.; Shionoya, M. Metal-mediated DNA base pairing: Alternatives to hydrogen-bonded Watson-Crick base pairs. *Acc. Chem. Res.* **2012**, *45*, 2066–2076. [CrossRef] [PubMed]
111. Tanaka, Y.; Oda, S.; Yamaguchi, H.; Kondo, Y.; Kojima, C.; Ono, A. 15N− 15N J-coupling across HgII: Direct observation of HgII-mediated T− T base pairs in a DNA duplex. *J. Am. Chem. Soc.* **2007**, *129*, 244–245. [CrossRef] [PubMed]
112. Park, K.S.; Jung, C.; Park, H.G. "Illusionary" polymerase activity triggered by metal ions: Use for molecular logic-gate operations. *Angew. Chem. Int. Ed. Engl.* **2010**, *49*, 9757–9760. [CrossRef] [PubMed]
113. Ono, A.; Torigoe, H.; Tanaka, Y.; Okamoto, I. Binding of metal ions by pyrimidine base pairs in DNA duplexes. *Chem. Soc. Rev.* **2011**, *40*, 5855–5866. [CrossRef] [PubMed]
114. Kuzuya, A.; Sakai, Y.; Yamazaki, T.; Xu, Y.; Komiyama, M. Nanomechanical DNA origami'single-molecule beacons' directly imaged by atomic force microscopy. *Nat. Commun.* **2011**, *2*, 449. [CrossRef]
115. Breaker, R.R.; Joyce, G.F. A DNA enzyme that cleaves RNA. *Chem. Bio.* **1994**, *1*, 223–229. [CrossRef]
116. Saran, R.; Liu, J. A Silver DNAzyme. *Anal. Chem.* **2016**, *88*, 4014–4020. [CrossRef]
117. Johnson, J.A.; Dehankar, A.; Winter, J.O.; Castro, C.E. Reciprocal Control of Hierarchical DNA Origami-Nanoparticle Assemblies. *Nano Lett.* **2019**, *19*, 8469–8475. [CrossRef]
118. Turek, V.A.; Chikkaraddy, R.; Cormier, S.; Stockham, B.; Ding, T.; Keyser, U.F.; Baumberg, J.J. Thermo-responsive actuation of a DNA origami flexor. *Adv. Funct. Mater.* **2018**, *28*, 1706410. [CrossRef]
119. Kou, B.; Chai, Y.; Yuan, Y.; Yuan, R. Dynamical regulation of enzyme cascade amplification by a regenerated DNA nanotweezer for ultrasensitive electrochemical DNA detection. *Anal. Chem.* **2018**, *90*, 10701–10706. [CrossRef]
120. Ketterer, P.; Willner, E.M.; Dietz, H. Nanoscale rotary apparatus formed from tight-fitting 3D DNA components. *Sci. Adv.* **2016**, *2*, e1501209. [CrossRef]
121. Wang, F.; Zhang, X.; Liu, X.; Fan, C.; Li, Q. Programming motions of DNA origami nanomachines. *Small* **2019**, *15*, e1900013. [CrossRef]
122. Cha, T.G.; Pan, J.; Chen, H.; Salgado, J.; Li, X.; Mao, C.; Choi, J.H. A synthetic DNA motor that transports nanoparticles along carbon nanotubes. *Nat. Nanotechnol.* **2014**, *9*, 39–43. [CrossRef]
123. Benson, E.; Marzo, R.C.; Bath, J.; Turberfield, A.J. A DNA molecular printer capable of programmable positioning and patterning in two dimensions. *Sci. Robot.* **2022**, *7*, eabn5459. [CrossRef] [PubMed]
124. Darcy, M.; Crocker, K.; Wang, Y.; Le, J.V.; Mohammadiroozbahani, G.; Abdelhamid, M.A.S.; Craggs, T.D.; Castro, C.E.; Bundschuh, R.; Poirier, M.G. High-force application by a nanoscale DNA force spectrometer. *ACS Nano* **2022**, *16*, 5682–5695. [CrossRef] [PubMed]
125. Wang, Z.; Song, L.; Liu, Q.; Tian, R.; Shang, Y.; Liu, F.; Liu, S.; Zhao, S.; Han, Z.; Sun, J.; et al. A tubular DNA nanodevice as a siRNA/chemo-drug co-delivery vehicle for combined cancer therapy. *Angew. Chem. Int. Ed. Engl.* **2021**, *60*, 2594–2598. [CrossRef] [PubMed]
126. Zhan, P.; Dutta, P.K.; Wang, P.; Song, G.; Dai, M.; Zhao, S.X.; Wang, Z.G.; Yin, P.; Zhang, W.; Ding, B.; et al. Reconfigurable three-dimensional gold nanorod plasmonic nanostructures organized on DNA origami tripod. *ACS Nano* **2017**, *11*, 1172–1179. [CrossRef]
127. Grossi, G.; Dalgaard Ebbesen Jepsen, M.; Kjems, J.; Andersen, E.S. Control of enzyme reactions by a reconfigurable DNA nanovault. *Nat. Commun.* **2017**, *8*, 992. [CrossRef]
128. Kroener, F.; Heerwig, A.; Kaiser, W.; Mertig, M.; Rant, U. Electrical Actuation of a DNA Origami Nanolever on an Electrode. *J. Am. Chem. Soc.* **2017**, *139*, 16510–16513. [CrossRef]
129. Liu, S.; Jiang, Q.; Zhao, X.; Zhao, R.; Wang, Y.; Wang, Y.; Liu, J.; Shang, Y.; Zhao, S.; Wu, T.; et al. A DNA nanodevice-based vaccine for cancer immunotherapy. *Nat. Mater.* **2021**, *20*, 421–430. [CrossRef]
130. Gerling, T.; Wagenbauer, K.F.; Neuner, A.M.; Dietz, H. Dynamic DNA devices and assemblies formed by shape-complementary, non–base pairing 3D components. *Science* **2015**, *347*, 1446–1452. [CrossRef]
131. Berg, H.C.; Anderson, R.A. Bacteria swim by rotating their flagellar filaments. *Nature* **1973**, *245*, 380–382. [CrossRef] [PubMed]
132. Boyer, P.D. The binding change mechanism for ATP synthase--some probabilities and possibilities. *Biochim. Biophys. Acta* **1993**, *1140*, 215–250. [CrossRef] [PubMed]
133. Noji, H.; Yasuda, R.; Yoshida, M.; Kinosita, K., Jr. Direct observation of the rotation of F1-ATPase. *Nature* **1997**, *386*, 299–302. [CrossRef]
134. Tomaru, T.; Suzuki, Y.; Kawamata, I.; Nomura, S.M.; Murata, S. Stepping operation of a rotary DNA origami device. *Chem. Commun.* **2017**, *53*, 7716–7719. [CrossRef] [PubMed]

135. Peil, A.; Xin, L.; Both, S.; Shen, L.; Ke, Y.; Weiss, T.; Zhan, P.; Liu, N. DNA assembly of modular components into a rotary nanodevice. *ACS Nano* **2022**, *16*, 5284–5291. [CrossRef]
136. Zhan, P.; Urban, M.J.; Both, S.; Duan, X.; Kuzyk, A.; Weiss, T.; Liu, N. DNA-assembled nanoarchitectures with multiple components in regulated and coordinated motion. *Sci. Adv.* **2019**, *5*, eaax6023. [CrossRef]
137. Marras, A.E.; Zhou, L.; Su, H.J.; Castro, C.E. Programmable motion of DNA origami mechanisms. *Proc. Natl. Acad. Sci. USA* **2015**, *112*, 713–718. [CrossRef]
138. Lee, A.J.; Endo, M.; Hobbs, J.K.; Walti, C. Direct single-molecule observation of mode and geometry of RecA-mediated homology search. *ACS Nano* **2018**, *12*, 272–278. [CrossRef]
139. Endo, M.; Katsuda, Y.; Hidaka, K.; Sugiyama, H. Regulation of DNA methylation using different tensions of double strands constructed in a defined DNA nanostructure. *J. Am. Chem. Soc.* **2010**, *132*, 1592–1597. [CrossRef]
140. Steinhauer, C.; Jungmann, R.; Sobey, T.L.; Simmel, F.C.; Tinnefeld, P. DNA origami as a nanoscopic ruler for super-resolution microscopy. *Angew. Chem. Int. Ed.* **2009**, *48*, 8870–8873. [CrossRef]
141. Schmied, J.J.; Raab, M.; Forthmann, C.; Pibiri, E.; Wunsch, B.; Dammeyer, T.; Tinnefeld, P. DNA origami-based standards for quantitative fluorescence microscopy. *Nat. Protoc.* **2014**, *9*, 1367–1391. [CrossRef]
142. Chandrasekaran, A.R. Nuclease resistance of DNA nanostructures. *Nat. Rev. Chem.* **2021**, *5*, 225–239. [CrossRef]
143. Perrault, S.D.; Shih, W.M. Virus-inspired membrane encapsulation of DNA nanostructures to achieve in vivo stability. *ACS Nano* **2014**, *8*, 5132–5140. [CrossRef] [PubMed]
144. Ponnuswamy, N.; Bastings, M.M.C.; Nathwani, B.; Ryu, J.H.; Chou, L.Y.T.; Vinther, M.; Li, W.A.; Anastassacos, F.M.; Mooney, D.J.; Shih, W.M. Oligolysine-based coating protects DNA nanostructures from low-salt denaturation and nuclease degradation. *Nat. Commun.* **2017**, *8*, 15654. [CrossRef] [PubMed]
145. Ijs, H.; Shen, B.; Heuer-Jungemann, A.; Keller, A.; Linko, V. Unraveling the interaction between doxorubicin and DNA origami nanostructures for customizable chemotherapeutic drug release. *Nucleic Acids Res.* **2021**, *49*, 3048–3062. [CrossRef] [PubMed]
146. Auvinen, H.; Zhang, H.; Nonappa; Kopilow, A.; Niemelä, E.H.; Nummelin, S.; Correia, A.; Santos, H.A.; Linko, V.; Kostiainen, M.A. Protein coating of DNA nanostructures for enhanced stability and immunocompatibility. *Adv. Healthcare Mater.* **2017**, *6*, 1700692. [CrossRef] [PubMed]
147. Ahmadi, Y.; De Llano, E.; Barisic, I. (Poly)cation-induced protection of conventional and wireframe DNA origami nanostructures. *Nanoscale* **2018**, *10*, 7494–7504. [CrossRef]
148. Agarwal, N.P.; Matthies, M.; Gür, F.N.; Osada, K.; Schmidt, T.L. Block copolymer micellization as a protection strategy for DNA origami. *Angew. Chem. Int. Ed.* **2017**, *56*, 5460–5464. [CrossRef]
149. Bujold, K.E.; Fakhoury, J.; Edwardson, T.G.W.; Carneiro, K.M.M.; Briard, J.N.; Godin, A.G.; Amrein, L.; Hamblin, G.D.; Panasci, L.C.; Wiseman, P.W. Sequence-responsive unzipping DNA cubes with tunable cellular uptake profiles. *Chem. Sci.* **2014**, *5*, 2449–2455. [CrossRef]
150. Wamhoff, E.C.; Romanov, A.; Huang, H.; Read, B.J.; Ginsburg, E.; Knappe, G.A.; Kim, H.M.; Farrell, N.P.; Irvine, D.J.; Bathe, M. Controlling nuclease degradation of wireframe DNA Origami with minor Groove Binders. *ACS Nano* **2022**, *16*, 8954–8966. [CrossRef]
151. Jahanban-Esfahlan, A.; Seidi, K.; Jaymand, M.; Schmidt, T.L.; Majdi, H.; Javaheri, T.; Jahanban-Esfahlan, R.; Zare, P. Dynamic DNA nanostructures in biomedicine: Beauty, utility and limits. *J. Control. Release* **2019**, *315*, 166–185. [CrossRef] [PubMed]
152. Coleridge, E.L.; Dunn, K.E. Assessing the cost-effectiveness of DNA origami nanostructures for targeted delivery of anti-cancer drugs to tumours. *Biomed. Phys. Expr.* **2020**, *6*, 065030. [CrossRef] [PubMed]
153. Praetorius, F.; Kick, B.; Behler, K.L.; Honemann, M.N.; Weuster-Botz, D.; Dietz, H. Biotechnological mass production of DNA origami. *Nature* **2017**, *552*, 84–87. [CrossRef] [PubMed]